The International Journal of Advanced Manufacturing Technology (2021) 112:655–684
https://doi.org/10.1007/s00170-020-06445-w

CRITICAL REVIEW

A review on micro-milling: recent advances and future trends

Barnabás Zoltán Balázs[1] · Norbert Geier[1] · Márton Takács[1] · J. Paulo Davim[2]

Received: 26 August 2020 / Accepted: 1 December 2020 / Published online: 28 December 2020

Abstract
Recently, mechanical micro-milling is one of the most promising micro-manufacturing processes for productive and accurate complex-feature generation in various materials including metals, ceramics, polymers and composites. The micro-milling technology is widely adapted already in many high-tech industrial sectors; however, its reliability and predictability require further developments. In this paper, micro-milling related recent results and developments are reviewed and discussed including micro-chip removal and micro-burr formation mechanisms, cutting forces, cutting temperature, vibrations, surface roughness, cutting fluids, workpiece materials, process monitoring, micro-tools and coatings, and process-modelling. Finally, possible future trends and research directions are highlighted in the micro-milling and micro-machining areas.

Keywords Micro-milling · Chip formation · Burr formation · Micro-milling tool

1 Introduction

Miniaturisation is a well-established recent demand of the industrial sectors, highly encouraged by the recommendations and laws of national governments and by the European Union (EU). Miniaturisation meets the recently published core missions and policy of the EU, like decreasing the negative effects of industrial processes on the climate change (product minimisation reduces the specific energy demand of the products) and increasing the number of smart systems and equipment in the cities and factories (smart systems and equipment require miniature parts like microprocessors and microcircuits) [1]. Therefore, the demand for miniature components has increased significantly in many areas of the industry, such as the aerospace, bioengineering, optics, microelectronics, automotive, medical and defence [2–6].

Miniaturised components can be manufactured by (i) electro-discharge machining [7–10], (ii) laser micro-manufacturing [11–13], (iii) lithography, electroplating and moulding (LIGA) [14, 15], (iv) deep reactive ion etching [16, 17], (v) deep UV lithography [18, 19] or (vi) mechanical micro-machining [20–24] technologies. Excellently precise geometrical features and small tolerances can be achieved by these micromachining technologies; however, their operation time and cost are often extremely high. Mechanical micro-machining is one of the most time-effective and most cost-effective methods for manufacturing miniaturised 3D components, mainly due to the relatively high material removal rate (MRR). Mechanical micro-machining processes can be categorized based on the analogy of the conventional-sized machining technologies: micro-milling, micro-drilling, micro-turning etc. One of the most commonly applied mechanical micro-machining technologies is the micro-milling [3, 4, 25–28]; this paper focuses therefore on its up-to-date review and discussion.

The main objective of the present paper is to review recent results and advances in micro-milling, including micro-chip removal and micro-burr formation mechanisms, cutting forces, cutting temperature, vibrations, surface roughness, cutting fluids, workpiece materials, process monitoring, micro-tools and coating, and process-modelling in order to summarise and discuss recent knowledge and outline possible future research directions and trends in micro-milling.

2 Micro-milling process

Micro-milling is a precise and flexible technology to manufacture complex 3D geometries in various types of materials

✉ Barnabás Zoltán Balázs
balazs@manuf.bme.hu

[1] Department of Manufacturing Science and Engineering, Faculty of Mechanical Engineering, Budapest University of Technology and Economics, Budapest, Hungary

[2] Department of Mechanical Engineering, University of Aveiro, Aveiro, Portugal

(metals and its alloys, polymers, ceramics, graphite, composites etc. [3, 26–38]) by relatively high material removal rates. The kinematic of micro-milling is similar to the conventional-sized milling process; however, there are some unique phenomena and key issues: (i) the size of the cutting tool can be extremely small (diameter of 25 μm [39] or 50 μm [40]), the length-to-diameter ratio is therefore often high. The unfavourable size of the tool, and the vibration and/or the relatively large tool run-out often lead to a tool-breakage [41]. (ii) The uncut chip thickness is often in the same order of magnitude as the cutting edge radius or as the grain size of the workpiece material [2, 32, 42, 43]. Therefore, the material deformation mechanisms are often dominated by the ploughing-effect [20, 44], and the quality of the surface is often inadequate [42, 45]. Furthermore, the value of the theoretical chip thickness is often similar to the size of the minimum chip thickness [20, 45, 46], which may prevent chip formation in each edge step-in [47, 48]. (iii) The ratio of the burr size to the size of the machined features is higher than it is used to in the case of the conventional machining operations, the cost and time needs of the micro-deburring processes have therefore more effect on the final cost of the products [49, 50]. Furthermore, it is extremely difficult to remove burr in micro-sized features [32, 51]. (iv) The stiffness, the attenuation and the accuracy of the micro-milling machine have a significant influence on the quality of parts. In addition, milling machines require extremely high spindle speeds (up to 450,000 rpm [52]) to grant proper cutting speeds. However, current micro-milling machine tool models provide often only maximum 200,000 rpm spindle speeds [53]. (v) The importance of the monitoring and diagnostics of micro-milling processes is sufficiently high because the cutting tool can easily damage the surface of the material (inappropriate surface roughness, burr formation, micro-crack formation etc.) or break [27, 54, 55]. Therefore, the monitoring of the tool-condition is highly recommended in the case of micro-machining processes. The aforementioned issues have been investigated by many researchers in the past years; however, there are still many lacks and challenges in this area [56–64], as discussed in the following chapters.

2.1 Chip removal mechanism in micro sizes

Chip removal mechanisms are mostly influenced by the material type (metallic materials, polymers, ceramics, composites or sandwich structures) and its properties, followed by the tool geometry (rake angle, cutting edge radius, clearance angle, diameter etc.), scale of machining (macro, micro, or nano) and the primary process parameters (cutting speed, feed rate, depth of cut) [56–66]. For example, the dominant chip removal mechanism for macro machining of a Ti6Al4V is shearing in the primary shearing zone [67], while the dominant chip removal mechanisms (CRMs) for macro machining of carbon fibre reinforced polymer (CFRP) composites are bending, delamination formation, crushing and shearing, depending mainly on the fibre cutting angle and tools' rake angle [68, 69]. However, if the above materials are machined in micro-scales, the ploughing dominates often the chip removal mechanisms [36].

In mechanical machining, the thickness of the removable material layer is limited; this limit is named as minimum chip thickness (h_{min}). If the undeformed chip thickness (h) is smaller than h_{min}, the cutting tool only compresses the top of the material instead of removing it. This phenomenon causes more often difficulties in micro-milling than in conventional-sized machining. According to Vipindas et al. [70], the cutting edge radius has the most significant influence on the size of the minimum chip thickness, as was confirmed by Wojciechowski et al. [47], Dib et al. [45], and Sahoo et al. [20] as well. The minimum chip thickness can be quasi-precisely estimated by an empiric model developed by Gao et al. [43] and Dib et al. [45].

As it is already discussed in depth by the researchers, the macro-chip removal mechanisms of quasi-homogeneous (e.g. metallic) materials are mostly shearing dominated [71], but the CRMs of micro-machining are often influenced mostly by the ploughing-effect, according to Aramcharoen and Mativenga [72]. Its reason can be found in the negative kinematical rake angle of the cutting tool, caused by the relative high cutting edge radius compared to the uncut chip thickness. The negative effective rake angle of the cutting edge compresses the top of the material, and it deforms plastically. The micro-chip removal mechanisms are illustrated in Fig. 1.

If the value of h is smaller than the value of h_{min} (Fig. 1a), the cutting tool presses only the material below the cutting edge, and it recovers back without any chip formation. In this case, the material deforms mostly elastically and it damages the surface structure (due to the plastic deformation), which results in worse surface quality [45]. If the value of h is comparable to the value of h_{min} (Fig. 1b), the chip starts to form due to the shearing effect in the primary shearing zone. In addition, the specific passive cutting force is high due to the relatively significant ploughing-effect. In the case of the h is greater than h_{min} (Fig. 1c), chip is continuously formed due to the stable plastic deformation in the shearing zone, while the elastically deformed material springs back. Nevertheless, the ratio of elastic recovery is lower. The undeformed chip thickness (h) is often thicker than the removed material depth [73]. This mechanism is the closest to the macro-chip removal mechanism of quasi-homogeneous materials.

The undeformed chip thickness is almost constant during orthogonal machining if the vibrations and the regenerative-effect is not considered. However, it is not constant during milling: its value is changing with the tool rotation; therefore, it may happen that all of the aforementioned cases (Fig. 1 a, b and c) appears and characterize the material removal process

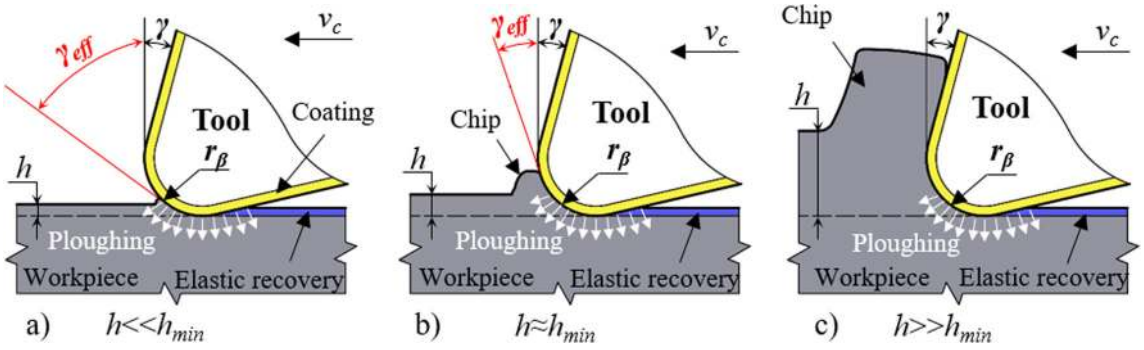

Fig. 1 Schematic of micro-chip removal mechanisms: (**a**) the undeformed chip thickness (h) is smaller than the minimum chip thickness (h_{min}), (**b**) the value of h is comparable to the value of h_{min}, (**c**) the value of h is higher than the value of h_{min} (adapted from [42, 72])

[25]. Furthermore, a low feed and/or a relatively high tool deflection may result in that chip not forms in certain cases, and the material is deformed elastically mainly [25, 47].

In mechanical micro-machining, the effect of the microstructure of the material (material defects; density, type, position, orientation and size of grains/fibres/particles) is significant [62, 74, 75]. The influences of the microstructure of an anisotropic and an inhomogeneous material are illustrated in Fig. 2. If the micro-particle (grain, fibre etc.) of the material is positioned completely below or above the theoretical cutting depth (Fig. 2a and b), the effect of the micro-particle is negligible. Nevertheless, the micro-particles have a significant effect on the CRMs if they are located in the depth of the theoretical cutting depth, as illustrated in Fig. 2c and d. The specific cutting energy demand of the micro-particles often higher than the matrix's [62], the pressing (Fig. 1c) or crushing (Fig. 1d) of the particles requires therefore more cutting energy, which may result in higher vibrations, faster tool wear, more burr formation and worse surface quality.

The deep technological knowledge and experience acquired in conventional-sized milling (macro-milling) cannot

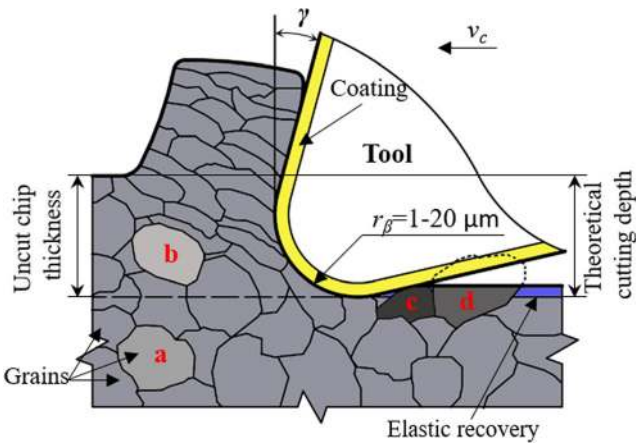

Fig. 2 Schematic of the influence of the position of particles on the micro-machining process: the micro-particle is positioned (a) completely below, (b) completely above, (c) close to and (d) on the level of the theoretical cutting depth (adapted from [42, 71, 72])

be directly applied to the micro-milling process, mainly, due to the size effect (the machining related phenomena and process characteristics are not correlated linearly with the tool's size-reduction) and the relative high tool deflections [25]. Therefore, the micro-chip removal mechanisms and the micro-milling of quasi-homogeneous materials were investigated previously by theoretical [76–78], experimental [42, 79–81] and simulation [80, 82, 83] approaches by many researchers. Bissacco et al. [84] investigated the limits of the size effect in micro-milling, which border separates the micro and macro-chip removal mechanisms. Aramcharoen and Mativenga [72] conducted micro-machining experiments on a hardened, very fine-grained H13 steel, and they found that the h_{min}/r_β ratio of the theoretical chip thickness (h) to the cutting edge radius (r_β) is a key parameter, which influences the micro-machining process significantly. According to their studies, the size effect is significant, when the ratio is less than 1. The cutting edge radius of a micro-milling tool is approximately 1–20 µm [39], which is about in the same magnitude as it is used at the conventional sized tools. The value of the cutting edge radius depends mainly on the material of the tool, the particle size, the manufacturing precision and the state of tool wear [74]. According to Bissacco et al. [25], the aforementioned h/r_β ratio has a great influence on the relative machining accuracy, burr formation and surface quality. Furthermore, the increasing of the feed per tooth (f_z) has a positive effect on the quality of machined features and also on the tool condition. Nevertheless, the optimisation process of the feed per tooth value should include the analysis of the cutting forces and the tool deflections.

Mian et al. [85] investigated the micro-machinability of an Inconel 718 alloy. They pointed out that nor only the ratio of f_z/r_β, but also the cutting speed is an important parameter from the point of view the size effect and the optimisation of the micro-milling process. In addition, they concluded that the specific cutting energy, the burr root thickness and the surface quality are recommended to be analysed in order to estimate the magnitude of the size effect. Pratap et al. [86] conducted micro-machining simulations on Ti6Al4V alloy and observed

that the size of stress in the primary shearing zone was relative high (2467 MPa), which was explained by the size effect.

Coatings can also be applied in the micro-machining technologies to increase tool performance and tool life, but it has to be pointed out that the thicker coating increases the value of the cutting edge radius, and thus affects minimum chip thickness [87]. Many researchers have studied the relationship between minimum chip thickness (h_{min}) and edge radius (r_β) using experimental [46, 88, 89], numerical [77, 90, 91], and analytical [92, 93] methods. For example, de Oliveira et al. [46] experimentally investigated the h_{min}/r_β ratio on an AISI 1045 steel and found that it changes between 0.22 and 0.36. Their observation was confirmed by Cuba Ramos et al. [88] and Kang et al. [89] on the same AISI 1045 material. The ratio of h_{min}/r_β was analysed in many materials and technologies; the calculated ratios are summarised in Table 1. As can be seen in the table, the ratio changes between 0.14 and 0.48. This ratio could indicate the goodness of technology or be a parameter which is monitored during the machining process. E.g. if the h_{min}/r_β gets smaller than a critical value, the cutting process parameters (or the cutting tool) has to be changed, in order not to reduce surface quality or machining efficiency.

2.2 Burr formation in micro sizes

One of the main micro-milling induced geometrical defects is the burr occurrence on the machined edges of the material. The specific size of the burr is usually smaller than it is used to observe in conventional sized milling; their removal is, therefore, more difficult and challenging task [32, 51]. The burr does not weaken the material; however, it greatly affects the quality of the part, as its size can be comparable to the diameter of the tool [98], and degrades its performance [32, 99].

Burr may be formed on the machined features of the material if the cutting tool plastically deforms the uncut material instead of removing them, which may be caused by the following main issues: (i) the uncut (theoretical) chip is not supported by any material or special supporting fixtures [100], (ii) the cutting edge radius and ploughing effect are relatively large [46, 101] (iii) the tool run-out is significant [46, 101], (iv) extensive and uncontrolled vibration (chatter) complicates the process [54, 82, 102], or (v) the type and position of the micro-particles of the part are unfavourable [62, 103]. Micro-groove-milling induced burr occurrence can be seen in Fig. 3. As it is clearly observable on the figure, the appearance of the burr on the top of the workpiece

Table 1 Summary of key papers dealing with the ratio of h_{min}/r_β

Authors	h_{min}/r_β	Material	Method	Response variables
Sahoo et al. [20]	0.25–0.33	P20 steel	Micro-milling, experimental	Surface quality, process signals
Wojciechowski et al. [47]	0.48	AISI 1045	Micro-milling, analytic-experimental	Cutting force
Dib et al. [45]	0.24–0.33	RSA 6061-T6	Micro-milling, experimental	Cutting force
Vipindas et al. [70]	0.33	Ti6Al4V	Micro-milling, experimental	Cutting force
Sun et al. [36]	0.4	Al7075-T6	Micro-milling, numerical	Cutting force and chip formation
Wang et al. [41]	0.3	Inconel 718	Micro-milling, numerical	Cutting force and chip formation
Aslantas et al. [94]	0.3	Ti6Al4V	Micro-milling, experimental	Cutting force, surface roughness
de Oliveira et al. [46]	0.22–0.36	AISI 1045	Micro-milling, experimental	Specific cutting force, surface roughness, chip formation
Ramos et al. [88]	0.29	AISI 1045	Orthogonal micro-turning, analytical and experimental	Surface roughness
Malekian et al. [92]	0.23	Al 6061	Micro-milling, analytical	Friction coefficient
Yang et al. [95]	0.4	Al 2024-T6	Micro-milling, numerical and experimental	Cutting temperature, cutting force, stress
Kang et al. [89]	0.3	AISI 1045	Micro-milling, experimental	Cutting force
Lai et al. [91]	0.2–0.4	OFHC copper	Micro-milling, numerical	Flow stress
Woon et al. [96]	0.26	AISI 4340	Micromachining, numerical	Shear stress, effective rake angle
Li et al. [81]	0.25	OFHC copper	Micro-milling, numerical and experimental	Surface roughness
Vogler et al. [90]	0.14–0.43	Ferrite-perlite steel	Micro-milling, numerical	Surface roughness
Liu et al. [77]	0.2–0.35	AISI 1040	Micro-milling, molecular-mechanical theory	Cutting temperature, shear stress, stress state
Liu et al. [77]	0.35–0.4	Al 6082-T6	Micro-milling, molecular-mechanical theory	Cutting temperature, shear stress, stress state
Son et al. [93]	0.2–0.4	Al, OFHC copper	Micromachining, analytical	Friction coefficient
Yuan et al. [97]	0.25–0.33	Cu–Mg–Mn aluminium alloy	Micro-turning, experimental	Cutting force, friction coefficient

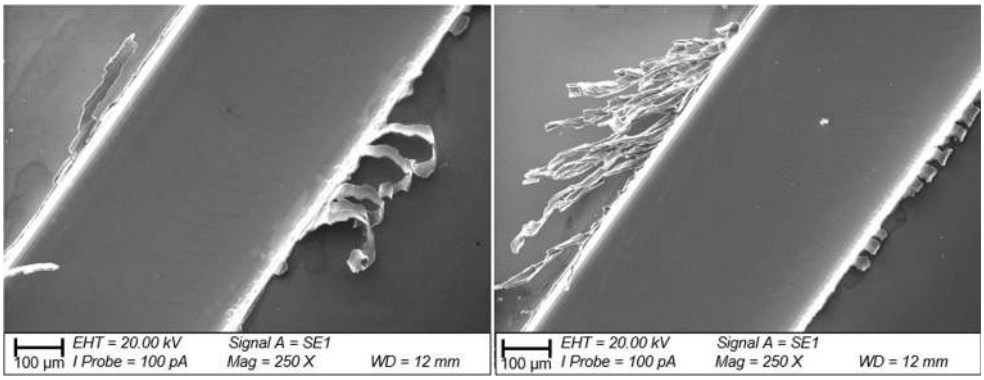

Fig. 3 Top burr on the micro-milled surface in AISI H13 (v_c = 90 m/min, a_p = 100 µm and (a) f_z = 2 µm, (b) f_z = 6 µm) [42]

material is significant, and its size is comparable to the size of the tool diameter. However, burr can be formed not only on the top edges of the material, but it is often observable on the entry and exit edges, too [78]. Figure 4 summarises the different burr types and their locations.

Three main burr formation mechanisms can be identified, which related to micro-milling processes [106]: (i) the material is compressed, mainly due to the ploughing effect, and it gets therefore bulged plastically to the sides of the material. This mechanism is named as Poisson (Fig. 5a). (ii) The uncut chip tearing from the material, rather than gets removed clearly. This mechanism is called as tear (Fig. 5b). (iii) The uncut chip gets bent rather than removed. This mechanism is named as rollover (Fig. 5c).

Burr formation is significantly influenced by the condition of the tool, which changes continuously as the cutting progresses. In order to select the appropriate parameters, it is important to know the actual condition of the tool [98], as the burr increases as the wear progresses [94, 98]. Oliaei and Karpat [108] examined the effect of the built-up edge on burr formation, but found no strong correlation; nevertheless, they found that higher forces result in a larger burr.

In the scientific literature, two main approaches can be found to eliminate burrs. The first one is to remove the burr after machining (deburring), and the other is to reduce it during machining. The latter approach is more appropriate in terms of machining costs and operation time; the optimisation of micro-milling processes is therefore essential. According to Saptaji and Subbiah [109], the incorrect design of deburring or incorrect selection of cutting parameters may cause a significant dimensional error, micro-damage, surface error, or residual stresses.

Many researchers have examined the effect of milling strategies on burr formation: the up-milling (also known as

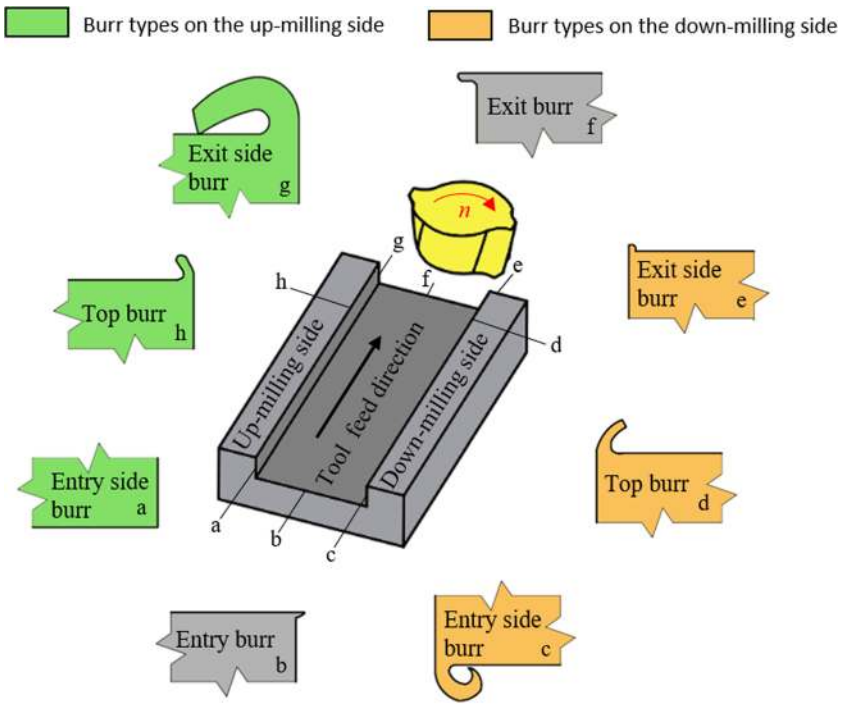

Fig. 4 Different burr types and their locations (adapted from [104, 105])

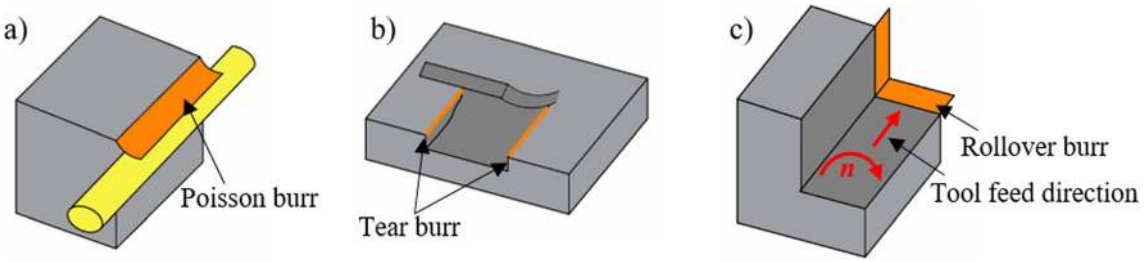

Fig. 5 The schematic of the (a) Poisson, (b) tear and (c) rollover burr mechanisms (redrawn [105, 107])

conventional milling) was to be found ideal from the point of view burr-minimisation on OFHC [110], Inconel 718 [85], Ti6Al4V [94], AA1100 [98], AISI 1045 [4], Al6061-T6 [109], X5CrNi18-10 [111] materials. Hajiahmadi [49] observed smaller top-burr height in the case of up-milling of AISI 316L, than it was observed at the down-milled (also known as climb milling) top edges. Nevertheless, the top-burr thickness was smaller at the down-milled edges. Piquard et al. [112] found a thinner and wider burr on the down-milled side.

Wu et al. [110] proposed an extra milling process with an up-milling strategy with a small width of cut to remove the formed burr. Mian et al. [85] observed that the burr-geometry—generated by the down-milling—is more uniform than the burr-geometry generated by the up-milling strategy. Biermann and Steiner [111] showed that the quality of the micro-machined side-wall of the workpiece is better when the down-milling strategy was applied; however, the burr-size was to be found larger, as was confirmed by Saptaji and Subbiah [109]. Mian et al. [85] proposed that the burr root thickness can be effectively controlled by the optimisation of the cutting speed and the ratio of the theoretical chip thickness to the edge radius. According to Kumar et al. [99], the cutting parameters, workpiece material properties, tool geometry, coatings, and coolant lubricants also affect the burr formation significantly in micro-milling. Piquard et al. [112] analysed the micro-milling process and found that the feed per tooth and the width of cut significantly affect the burr size. They also found that higher feed per tooth and smaller cutting width values have a positive effect on the burr formation mechanisms.

Aramcharoen and Mativenga [72] experienced a decreasing burr size on hardened H13 steel, as the ratio between the undeformed chip thickness and the cutting edge radius increased. They explained it by the decreasing ploughing phenomenon. Chen et al. [113] proposed to decrease the ratio of depth of cut to tool diameter in order to minimise burr formation. Increasing the cutting speed and feed per tooth also had a positive effect on burr formation in the parameter ranges v_c = 40–90 m/min and f_z = 1–4 μm [4]. Kumar et al. [32] examined the lateral exit-burr and found that it is unfavourable at the up-milled sides. Nevertheless, Kiswanto et al. [98] observed significant exit-burr formation at the down-milled sides as well. Furthermore, they could not found any significant differences between the burr-shapes at the up-milled and down-milled sides. Gilbin et al. [29] conducted micro-milling experiments on 42NiCrMo16 using a diameter of 500 μm end mill. They showed that an increase in feed was found to be the most suitable for reducing the exit burr, while unlike in macro-milling, this did not have a significant effect on surface quality. In contrast, according to Biermann and Steiner [111], increasing the feed may cause a higher top burr height in X5CrNi18-10, possibly because the increased amount of material cannot be removed continuously with only a single cut. They also concluded that increasing cutting speed due to "the higher strain rate hardening of material", and the use of sharp tools with a positive rake angle and a large spiral angle is advantageous to reduce the size of the upper burr.

Kumar et al. [32] studied the micro-machinability of Ti6Al4V and they could decrease the height of exit-burr by reducing the cutting speed from 314 m/min to 79 m/min. Aramcharoen et al. [2] micro-machined AISI H13 and observed that most of the tool coatings are suitable for reducing the size of burrs. Swain et al. [79] conducted micro-machining experiments on Nimonic 75 alloy and compared the cutting-ability of a nanostructured TiAlN coated tool and an uncoated one. They found that the tools perform almost identically at the start of the cutting, but with increasing the cutting length—due to the different wear behaviours—the burr increases more rapidly in the case of the uncoated cutting tool is applied.

According to Komatsu et al. [114], by reducing the grain size of the material, the size of the burr can be reduced. For normal grain sizes (~ 9.10 μm) the cutting force suddenly decreases at the end of the cut with the variable primary shear angle, and a large burr forms at the edges. In contrast, in the case of ultrafine grain materials, (~ 1.52 μm), the force reduction at the end of the chip separation takes place gradually. Wu et al. [110] conducted finite element and experimental investigations on an oxygen-free copper using a diamond tool and pointed out that the Poisson burr is caused by the lateral flow of stagnant material at the lower segment of the cutting edge. During their investigation, the cutting edge radii were set to 0, 1, 2 and 5 micrometres, which parameters were smaller and also higher than the uncut chip thickness. They observed that the area of the maximum stress shifted from the upper corner of the cutting edge to the lower corner, due to the dominant ploughing effect. All of these resulted in larger Poisson burr.

According to the authors, the burr formation is minimal, if the uncut chip thickness is reduced to the same value than the cutting edge radius. However, the further decrease in the chip thickness induced an opposite effect. According to Aurich et al. [40], a tilted spindle results in a completely different material removal condition than the conventional one. Due to the tilted cutting tool, the effective helix angle can be minimised, which may have a positive effect on burr formation. Kou et al. [115] recommended the use of adhesive supporting material to increase the stiffness of the edge of the workpiece. In the case of their novel method, the burr is formed on the supporting material, which can be removed from the piece more easily. The procedure was experimentally verified. Saptaji et al. [109, 116] proved that tapered tools could reduce the top burr as well as the exit burr due to the sloping walls. They recommended a diamond single crystal tool with a very small cutting edge radius for ductile materials to reduce burrs, which require high accuracy and good vibration control for efficient use additionally.

2.3 Cutting force in micro-milling

The main differences between macro and micro-scaled machining from the point of view cutting force can be seen in Fig. 6. Due to the size reduction in micro-milling, the magnitude of the cutting forces is significantly smaller than in the case of macro-milling. Typically, the force amplitudes are between a few tenths and a few tens of Newtons. Nevertheless, the ratio of cutting force (F_c) to the passive force (F_p) differs significantly. In the case of micro-milling, the passive force has a more significant effect on the chip removal process, which is a consequence of the ploughing phenomenon.

It is essential to know and monitor the cutting forces because they provide information about many phenomena, such as chip formation, mechanism of material removal, vibration, and tool condition [68, 74, 118]. All of these contribute to improving the predictability of the process, reducing the speed of the tool wear and increasing the reliability of the process.

As discussed earlier, in the case of micro-milling, the cutting edge radius plays an important role in the chip removal because it affects the minimum chip thickness, as well as the material removal mechanisms. Since the value of r_β and other characteristics of the tool are constantly changing due to tool wear, the effect of wear on cutting forces is the subject of many researches [76, 94]. Afazov et al. [119] micro-milled AISI 4340 steel and proved that higher cutting edge radius causes higher cutting forces. Wu et al. [120] machined OFHC copper and found that the ratio of shear force and ploughing force to the main cutting force was 55% and 45%, respectively. As the radius increases, the difference is shown here also increases. Yang et al. [95] conducted micro-milling experiments on Al2024-T6 aluminium alloy and showed that although the cutting forces are higher, the effective stress reduces. Pratap et al. [86] analysed the cutting forces during micro-milling of Ti6Al4V alloy. They found that higher cutting forces are caused by mainly the accelerated tool wear rates (~ higher cutting edge radius), caused by the increased cutting temperatures. In this scenario, the increase in force is due to the stronger ploughing phenomenon, which occurs when the value of the chip thickness is below the value of minimum chip thickness [91, 121]. All of these phenomena often contribute to unpredictable tool life [87]. Mian et al. [85] pointed out that at small theoretical chip thickness, the ploughing effect is present for a longer time until the tool actually starts to cut. At higher feed per tooth values, the dominance of the ploughing effect is often reduced.

A significant increase in the specific cutting force is observed at small chip thicknesses due to the phenomenon of the size effect [122]. According to Gao et al. [43], a larger cutting edge radius results in a larger negative rake angle, which affects the shear and ploughing force significantly. The ploughing force increases significantly below the minimum chip thickness, which also entails a significant increase in the specific cutting force. In micro-milling, forces can also increase due to the excessive reduction in feed rate due to the ploughing phenomenon. Aslantas et al. [94] showed that a tool with a low coefficient of friction could prevent

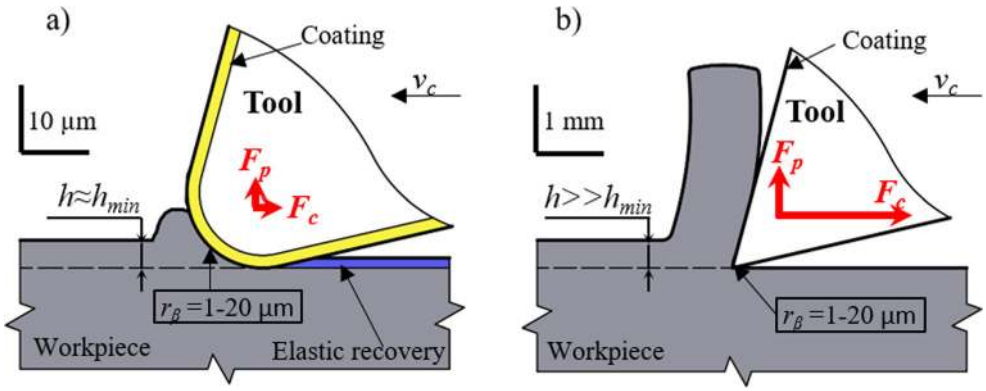

Fig. 6 Dominant cutting forces in (a) micro-milling and in (b) macro-milling, where F_p denotes the passive force, F_c the cutting force (adapted from [71, 117])

ploughing. Lu et al. [76] developed a novel cutting force model, which gives an accurate estimate of the forces taking into account the wear state of the tool. de Oliveira et al. [46] studied the effect of the feed per tooth on the specific cutting force at macro and micro-sized milling operations. In the case of micro-milling, specific cutting force by an average of 22% could be reduced by doubling the feed per tooth; and it could be reduced by 13% by doubling the depth of cut. These values were only 18% and 7% in macro sizes, respectively. Similar trends were observed in 12Cr18Ni9 by Gao et al. [43], and it was shown that increasing the cutting width (a_e) also reduces the specific cutting force.

Zhou et al. [123] performed micro-milling simulations on NAK80 steel, and found that the effect of cutting speed on cutting forces is negligible in their studied parameter range (v_c = 12–36 m/min, f_z = 0.3–12 μm). Wang et al. [41] micro-milled Inconel 718 alloy, and showed that the cutting force increases with increasing feed per tooth and a_e. They also highlighted, that the feed per tooth should be set above a critical value (h_{min}), and the a_e should be chosen relatively small to reduce the forces. Sun et al. [36] conducted 3D finite element micro-milling simulations on Al7075-T6 alloy, and observed that higher cutting width results in higher cutting forces. According to Komatsu et al. [114], the ratio of force components (Z to X) is higher in the case of ultrafine grain steels than at normal grain sizes. The shear force decreases with ultrafine grain materials while the friction force increases. Ahmadi et al. [124] also observed higher forces for smaller grain sizes. The cutting forces depend significantly also on the milling strategies: the forces are usually lower for up-milling than for down-milling in AISI 1045 steel [38].

2.4 Cutting temperature in micro-milling

Cutting temperature plays an important role in all of metal cutting processes as it significantly affects tool wear, burr formation, chip removal mechanisms, and the surface quality [95, 125]. According to the study made by Mamedov and Lazoglu [126], cutting temperature also has a direct effect on residual stresses, 3D distortions, and dimensional accuracy of the machined micro-features. Wissmiller and Pfefferkorn [125] pointed out that thermal expansion plays a significant role in this size range, not as negligible as in the case of conventional-sized machining operations. Yang et al. [95] conducted micro-milling experiments on Al2024-T6 alloy and analysed the cutting temperature. They found that only a small part of the generated heat is concentrated on the contact between the tool and the workpiece. It was observed that the maximum temperature field extends from the rake face through the corner of the cutting edge to the flank face, as illustrated in Fig. 7.

Wissmiller and Pfefferkorn [125] investigated the geometry of cutting tools and found that shorter edges and shorter transition sections allow better thermal conduction, thus reduced the maximum tool temperature. Mamedov and Lazoglu [126] conducted micro-milling simulations and found that the temperatures increased with the chip load. Thus, increasing the feed leads to an increase in temperatures, as was confirmed by Wissmiller and Pfefferkorn [125]. In addition, higher depth of cut values results in higher cutting temperatures [126]. Nevertheless, the low feed per tooth—which mainly results in plastic deformation on the workpiece surface—can results in higher temperature and adhesive wear, according to Uhlmann et al. [128].

The measurement of cutting temperature during the micro-milling process is extremely challenging, therefore, many researchers investigated it by simulations. Yang et al. [95] simulated micro-milling process on Al2024-T6 alloy and found that increasing the radius of the cutting edge (0; 3.2; 5; 7 μm), the tool temperature decreases (57.5 °C; 51.5 °C; 45.4 °C; 40.4 °C, respectively). The temperatures obtained here were low compared to conventional sized milling. Balázs and Takács [83] observed similar results: the results of the finite element simulations of the thin chip removal process showed that the tool

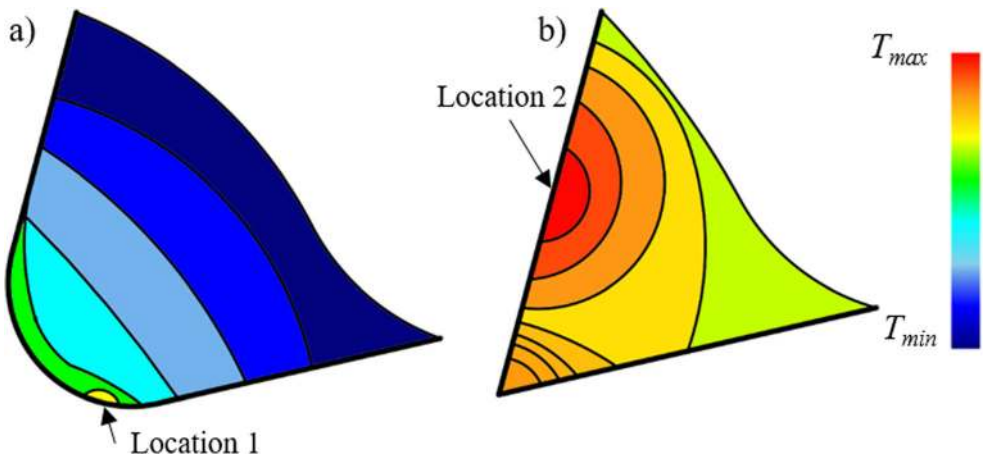

Fig. 7 Cutting temperature zones in (a) micro-machining and (b) macro-machining (adapted from [71, 127])

temperature is quite low at machining of AISI 1045 steel. According to the authors, the increase of both feed per tooth and cutting speed result in increased tool temperature.

Wissmiller and Pfefferkorn [125] simulated the micro-milling of AISI 1018 steel and resulted in a tool temperature of 91.85 °C at v_c = 37.68 m/min and v_f = 200 mm/min, while 49.85 °C tool temperature resulted in Al 6061-T6 alloy at v_c = 37.68 m/min and v_f = 700 mm/min. Despite the fact that the feed is lower in the case of steel than in the case of aluminium alloy, this is not an unexpected result, as the yield-strength of steel is much higher than that of the aluminium alloy. Pratap et al. [86] conducted finite element micro-milling simulations on Ti6Al4V material, and a maximum temperature value of 845.3 °C was determined with the parameters v_c = 31.415 m/min, f_z = 1 µm and a_p = 30 µm. Thepsonthi and Özel [129] simulated micro-milling of Ti6Al4V and found that the cutting temperature could reach 420 °C. Based on the simulations made by Zhou et al. [123] the highest temperature occurred in the secondary shear zone (210 °C) on NAK80 mirror die steel. Biermann and Steiner [111] did not experience thermally induced softening in austenitic stainless steel even at higher cutting speeds, which may be due to the very short contact time between the workpiece and the tool.

In summary, studying the cutting temperature in micro-milling is not a very extremely investigated topic, as it is a very challenging process. The characterising temperatures of micro-machining are typically lower than in the case of conventional-sized machining. The maximum temperature of the micro-sized tool is typically below 100 °C.

2.5 Vibrations in micro-milling

Minimization of tool vibration is one of the main challenges in conventional sized milling processes because inappropriate vibration (chatter) often results in accelerated tool wear or poor surface quality [130–132]. In addition to these difficulties, chatter may cause tool breakage in micro-milling [82, 133]. Due to the size reduction, the micro-milling process requires small-diameter tools (slender tools), and their stiffness is therefore often one order of magnitude lower than those used in conventional sizes. This limited stiffness is a major obstacle, when machining difficult-to-cut materials, such as hardened steels and titanium alloys [134]. In addition to the low stiffness of the tools, the high specific cutting force—at small depth of cut values—also makes the optimization of the micro-milling process more difficult [135]. However, the stability of the micro-milling process can be improved by (i) the increased process damping due to the ploughing phenomenon, and by (ii) the increased contact area of the clearance surface and the workpiece [102, 136]. Cutting tool vibration can be modelled using springs and attenuations [137–139]. Figure 8 compares the macro and micro-cutting processes from the point of view vibration characteristics. As it can be seen in the figure, the ratio of cutting force to the passive force (F_c/F_p) is usually smaller in micro-cutting than in conventional sized cutting, the vibration in the direction of the cutting speed is therefore relatively smaller, and the vibration in the direction of the depth of cut is relatively higher in micro-cutting.

Mittal et al. [5] stated that limited stiffness is one of the main obstacles, when machining difficult-to-cut materials (such as Ti6Al4V). However, this property characteristic can be improved by using high cutting speeds because the cutting forces decrease at higher speeds, caused mainly by the reduced chip load. Although, at high cutting speeds, dynamic changes in cutting forces can make the process unstable. In this case, the heat generation may also be higher, which, combined with the poor thermal conductivity of the workpiece material (e.g. in polymers), also affects the forces and unstable behaviour. Gilbin et al. [29] stated that the low stiffness of the tools also plays a role in the development of dynamic phenomena and significant deflection. They confirmed that the stabilisation of the tool and cutting process could be achieved by increasing speeds. Singh et al. [134] also stated that the chip load should be reduced in the case of high speeds, but this may result in an intensification of the ploughing

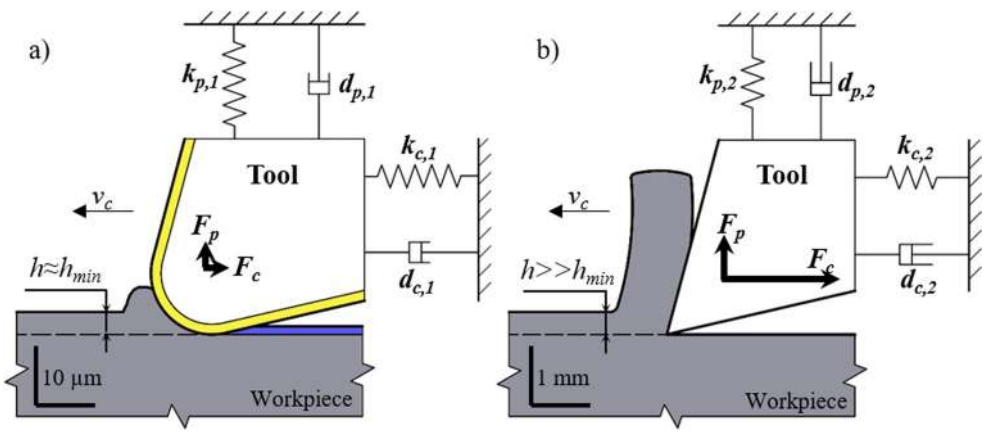

Fig. 8 Comparison of mechanical models of (a) micro and (b) macro-sized machining (k denotes the spring constant and d the damping constant) (adapted from [5, 139])

phenomenon, which can result in even an order of magnitude higher vibrations.

As it is well-known, vibrations and chatter often cause poor surface quality and tool failure due to unstable cutting conditions [37, 38, 134, 140]. Considering the special characteristics of the micro-milling process, such as the (i) small diameter of tool (< 1 mm), (ii) relatively large tool run-out and (iii) deformations; it can be concluded that the dynamic behaviour of the process is extremely complex [38]. The most common form of self-excited vibration is the regenerative chatter, which causes instability in the cutting process [5]. This is one of the main obstacles to improving productivity and component quality [141].

Takács et al. [38] demonstrated the presence of strong vibration in the AISI 1045 micromachining through a characteristic pattern left on the surface and through fast Fourier transformation (FFT) analysis. A similar case can be seen in the study of Singh et al. [134]. According to Biermann and Baschin [140], due to the small theoretical chip thickness and the effect of the cutting edge on chip formation, the regenerative effects are stronger than at macro sizes. The authors emphasise the importance of analysing the cutting forces in order to control vibrations, deformations and other errors caused by the low rigidity of the tool. Reducing the feed per tooth in micro-sizes is not advantageous, as it also changes the uncut chip thickness, which has a non-linear relationship with the cutting forces. According to Mamedov et al. [142], great emphasis should also be placed on the analysis of cutting forces in the study of the mechanics and dynamics of the micro-milling process.

Jun et al. [143] presented a dynamic micro-milling model for predicting cutting forces and vibrations, which also takes into account spindle errors and cutting tool defects. According to Moges et al. [3], the instantaneous uncut chip thickness associated with the cutting edge, which offset is the longest (compared to the other edges), is greatly influenced by the tool run-out. Furthermore, this longest-offset-edge often gets a significantly higher load and the other edge may not enter the workpiece or the edge impact's time is shorter. The difference in chip load is greater at lower feed per tooth. According to the authors, in order to accurately predict the geometrical parameters of the process, in addition to the tool run-out, the relationship of the current path of the tool edge with the trajectory of several preceding tool edges must be taken into account. Furthermore, the elastic spring-back of the workpiece also has a significant effect on the process characteristics, when the chip thickness is below the $h_{\min}$ value. According to Biermann and Baschin [140], a small corner radius (~ 0.1 mm) can have a beneficial effect on the vibrational trajectories of the tool and on the reproducibility of the process. The right selection of tool radius is also important because it significantly affects the minimum chip thickness. In addition, the tool wear, the tool finishing process (which is often grinding), and the coating process also affect the condition and stability behaviour of the cutting edge.

Yilmaz et al. [37] studied the dynamics of a micro-milling tool. Their presented method is based on an inverse stability analysis, where the modal parameters are updated with the results obtained from the chatter-tests to bring even closer the dynamic behaviour of tool centre point (TCP). Stability diagrams require FRF (frequency response function) analysis of the TCP, which cannot be determined experimentally due to the small tool size, so an analytical approach has been presented by the authors [37]. Singh and Singh [82] also examined tool dynamics. Finite element modal analysis was used to determine FRF, and the results were validated experimentally. The difference between the two methods in the first mode natural frequency was 6.6%. Based on their studies, the first mode natural frequency was 4851 Hz, the second 5081 Hz, and the third 7170 Hz. In contrast to the data presented above, Takács [74] found the natural frequency value of bending no. 1 to be more than 250,000 Hz for similar *l*/*d* ratio's tools.

The determination of stability curves also plays an important role in stable chip removal conditions and it is, therefore, the subject of much research works. Afazov et al. [119] studied stability limits on AISI 4340 steel. In the study of the effect of rake angles, lower stability limits, as well as higher forces, were observed at a rake angle of 0° than at 8°. The increase in cutting forces and the decrease in stability limits are much stronger for small cutting edge radiuses and large theoretical chip thicknesses. According to the authors' study, the stability limits can be increased by preheating the workpiece to 600 °C, which leads to softening of the workpiece, thereby reducing the cutting forces. In another study, the same authors presented a vibration model, where they found that modal-dynamic parameters have a significant effect on stability curves, especially above 35,000 rpm (v_c = ~ 55 m/min). With increasing tool run-out, as well as increasing feed per tooth, the stability area decreases linearly due to higher forces [139].

Singh et al. [134] modelled the dynamic stability of the micro-milling process in Ti6Al4V. The estimated and measured stability limits up to 70,000 rpm show a good agreement, but differ significantly above it. The differences are explained by the authors with decreasing damping at high speeds and the Coriolis-effect due to rotational and vibrational movements. Mokhtari et al. [144] presented a novel method to study the unstable vibrational behaviour of micro-milling. Their studies took into account the size effect, the gyroscopic moment, the rotary inertia, the structural nonlinearities and process damping. Sahoo et al. [145] proposed an analytical approach to study cutting forces and dynamic stability. They combined the finite element modelling with mechanical modelling, which also takes into account tool run-out, minimum chip thickness, elastic recovery, and the ploughing phenomenon. Mittal et al. [5] conducted micro-milling experiments on Ti6Al4V and found, that a transition at

47,000 rpm was clearly demonstrated from the cutting force data, where the process becomes lubrication-sensitive.

2.6 The surface roughness of micro-milled geometrical features

One of the critical quality characteristics of micro-machined components is the surface quality, so a large area of research focuses on how factors affect it. Uhlmann et al. [146] conducted micro-milling experiments on X13NiMnCuAl4-2-1-1 and found that the cutting edge radius significantly influences the surface roughness of the machined part. Aramcharoen and Mativenga [72] experienced the best surface quality on a very fine-grained AISI H13, when the uncut chip thickness and the tool radius of the cutting edge were set to the same value. Li and Chou [147] found that surface quality is closely related to the wear state of the tool in SKD 61 (38 HRC). It is well-known, that, as the cutting progresses, the edge rounding increases [95]. According to Zhu and Yu [27], the tool wear also affects surface integrity and product geometry. Oliaei and Karpat [108] analysed micro-machinability of Ti6Al4V and found that the increasing cutting speed does not improve the surface quality. Li and Chou [147] found on SKD 61 that neither the cutting speed nor the feed (v_c = ~ 37.5–75.4 m/min, f_z = 1–2 μm) had a significant effect on surface quality. Kiswanto et al. [98] studied the micro-milling process with statistical methods, with particular regard to productivity, and suggested that the use of higher feed rates is recommended as it does not degrade surface quality significantly (investigated parameter ranges v_c = ~ 22–59.7 m/min, f = 0.05–1 mm/s).

Mian et al. [85] examined surface roughness results by means of analysis of variance (ANOVA). In contrast to the previously discussed studies, it was found that in addition to the ratio of the theoretical chip thickness to the edge radius, the cutting speed also has a significant effect on the surface roughness. It was found that the cutting speed was the most significant parameter to improve surface quality. Uhlmann et al. [128] analysed micro-milling in WCu. They observed that the surface roughness increases with decreasing cutting speed, which may be caused by the formation of a built-up edge. It was found that increasing the feed per tooth leads to (i) geometric inaccuracy and (ii) higher abrasive wear, which causes the cutting edge to round, as well as increasing the plastic deformation on the workpiece surface. An improvement in surface quality was achieved with increased cutting speed.

According to Zhang et al. [148], the low stiffness of the tool during the micro-milling process is one of the biggest obstacles in terms of surface quality. Cutting forces result in considerable tool deformations, which affect the quality of the machined surfaces, as it is proved by Mamedov et al. [142]. Ahmadi et al. [124] found slightly better surface quality in Ti6Al4V in the case of finer grain sizes of workpiece material. Oliaeia and Karpat [149] micro-milled Stavax stainless steel. It was found that each different cutting width (a_e) values have a preferred feed per tooth value. Lower a_e values result in lower surface roughness. With larger cutting width values, the surface quality is better at higher feed per tooth values. An optimum was found at a_e = 20% and f_z = 4 μm.

Bissacco et al. [84] studied micro-milled surfaces in detail. The cutter marks on the surface are related to the geometry of the tool and also includes the accumulation of plastically deformed material. In the other case, there is a smear of the material behind the tool, which generates small waves in the feed direction. Because of these effects, surface roughness can only be reduced to a limited value by reducing the tool diameter. In the study of milling strategies in Ti6Al4V by Ahmadi et al. [124], based on analyses with EBSD, up and down-milling strategies resulted in a different surface texture. It was observed that greater compressive deformation occurs in down-milling than in the up-milling. Aurich et al. [40] investigated the effect of the spindle tilting angle, and based on their experiments, tilting the tool also degrades surface quality and geometry. The significant differences between their simulated results and their experiments can be traced back to the ploughing effect, which is significant in micro-milling.

Wang et al. [150] studied the surface characteristics at different stages of tool wear on Ti6Al4V. Based on their investigations, the main forms of surface defects are: feed marks, material debris, plastic side flow and material smears. As wear progressed, mainly material debris and plastic side flow became more significant. Meanwhile, the surface quality on the up-milled side was better than on the down-milled side. According to K and Mathew's [151] micro-milling studies in Ti6Al4V (using 3–3.5 μm cutting edge-rounding and a TiAlN coated cutting tool), as the wear progressed, the surface roughness decreased at a feed rate of f_z = 5 μm per tooth, and the roughness value has a minimum at 700 mm machined length. In contrast, at f_z = 0.3 μm, the roughness increased with the cutting length. The authors recommended to set the feed per tooth to a slightly higher value than the cutting edge radius in order to optimise surface roughness.

2.7 Application of cutting fluid in micro-milling

One of the main purposes of using cooling lubricants is to increase the quality of machined parts and the economy of machining. The use of coolants and lubricants in macro sizes improves the surface quality, has a positive effect on tool wear and cutting forces [71, 73]. Cutting fluids can be used to reduce thermal deformations, which also contributes to geometrical accuracy, as well as chip removal [71, 73, 127]. A significant challenge with coolants is that they are harmful to the environment and human health. Therefore, nowadays, environmentally friendly methods such as dry cutting, minimum quantity lubrication (MQL), nanofluid minimum quantity lubrication and cryogenic cooling are getting more popular [152–154]. There

are a lot of researches going on to investigate the effect of coolants and lubricants on a micro-scale machining.

According to Li and Chou's [147] micro-groove-milling experiments on SKD 61, even a small amount of oil (1.88 ml/h) proved to be sufficient for minimum quantity lubrication, the required air volume was found in 40 l/min. Oil is required to achieve a long tool life; just using clean air alone does not increase tool life [147]. Ziberov et al. [155] performed micro-milling experiments on Ti6Al4V material and observed that the wear behaviour of the tools differs significantly at MQL compared to dry machining. In the former, the secondary clearance surface was mainly worn, while in dry conditions, cutting edge rounding increased more. In the case of dry machining, the tool life was longer, reaching the wear criterion after more than twice the cutting length ($l_c = 21.0$ and 50.4 mm). This may be explained by the built-up edge that protected the tool. In contrast, in the study made by Li and Chou [147], it was found that the flank wear reduced to 60%, when MQL was applied, compared to dry machining.

Kumar et al. [99] conducted micro-milling experiments and found that coolant-lubricating fluids also influence significantly burr formation not only cutting temperature or tool wear speed. Li and Chou [147] performed micro-milling experiments on SKD 61 steel and found that MQL has a beneficial effect on burr formation due to less tool wear. On the other hand, Ziberov et al. [155] measured higher top burr heights in Ti6Al4V material with MQL. In dry conditions, the burr was larger on the down-milling side, but at the minimum quantity lubrication, the milling strategies did not show a significant difference in this respect. Biermann and Steiner [111] micro-milled X5CrNi18-10, and showed an increase in the height of the top burr when using MQL, in contrast, flood lubrication and bath lubrication had a positive effect. The MQL has a favourable effect on the surface quality [147, 155].

Aslantas et al. [156] studied a newly designed hybrid cooling lubrication system and based on their experiments on Ti6Al4V, air at − 10 °C showed a favourable effect with minimum quantity lubrication. However, a colder air (− 30 °C) had a negative effect on tool wear and burr formation due to excessive chip formation. As the cutting length increased, no significant change in burr size was found, which can be a significant advantage for micro-milling. In addition, they measured the lowest R_a value at dry machining. According to Kim et al. [152], in the micro-milling of Ti6Al4V, nano-sized diamond grains (35 nm) and cold (− 25 °C, pressure 0.15 MPa) CO_2 gas mixed in the minimum quantity lubrication (vegetable oil was the base lubricant) are effective solutions for reducing cutting forces, tool wear, the coefficient of friction and improve the surface quality. While the first three require a lower concentration of "nanodiamond" in the nanofluid (~ 0.1 wt.%), a higher concentration (1.0 wt.%) is required to improve surface roughness. Mittal et al. [5] investigated the effect of different lubricants on the dynamic behaviour of the micro-milling process. A significant improvement in stability limits was observed with lubrication in Ti6Al4V, showing a 20% increase at 100,000 rpm. In addition, a limit speed has been established, below which the process is insensitive, above which it is already sensitive to lubrication.

2.8 Micro-milled workpiece materials

The versatility of micro-milling is demonstrated not only by the complex geometries, but also by the wide range of machinable materials. In this chapter, the most important material characteristics, as well as the special materials and their applicability, are collected.

According to Komatsu et al. [114], smaller grain sizes are required for higher machining accuracy because the grain size is relatively large to the depth of cut in the case of micro-milling. Bissacco et al. [25] also suggested the application of workpieces with small grain sizes, and highlighted the importance of homogeneity of workpieces. According to the research work of Mian et al. [85], if the theoretical chip thickness falls below the cutting edge radius or grain size, the material of the workpiece greatly influences the chip formation, deformation mechanism and flow. Wu et al. [120] analysed micro-machinability of copper and found that forces and specific energy are also higher at smaller grain sizes. This was explained by the fact that the cutting takes place by the movement of the dislocations, which are inhibited at the micro-scale by the grain boundaries. Smaller grain sizes have longer specific grain boundaries, which means a greater inhibitory effect. Based on their results, the effect of grain size is smaller than that of the edge radius.

Micro-machining researches are carried out in a wide range of materials, with a very significant proportion of the research being steels, which is the most widely used metal in the engineering world. For the sake of example, many researchers studied micro-machinability of AISI 1045 (partly as reference material) [4, 38, 46, 77, 88], different stainless steels [43, 84, 114], and also hardened steels [29, 30, 84, 157]. Several researchers have also investigated aluminium micromachining [95, 109, 125, 142]. The Al7075-T6 is widely used in the aerospace industry because its specific material properties are excellent: it has a good volume-to-weight ratio, high strength and toughness and antioxidant [36]. Copper micromachining is also a highly researched field [40, 102, 110, 120]. Inconel 718 [41, 85, 158–160], a nickel-based superalloy, has been reported in several publications. It is characterised by a stable structure, high hardness, high deformation resistance, good chemical stability, as well as resistance to heat and corrosion [41]. They are often used in the aerospace industry, pressure vessels, armarioum ocean and pollution control [161]. Hard-to-cut materials can typically be machined at low cutting speeds, but this makes it difficult to reconcile their machining with efficiency and economy [41].

Researchers investigated WCu micro-milling also, which is difficult-to-machine due to its microstructural properties, for example, due to the quality of the material used as an electrode for electrical-discharge machining (EDM) [128]. Many studies are also performed on titanium and its alloys [5, 32, 35, 94], which are typically used in the aerospace industry, space research, biomedical devices, and medicine [32, 35, 40, 162, 163]. It has several favourable properties such as high strength, corrosion resistance and biocompatibility [35, 124], but they belong to the group of difficult-to-cut materials [126]. Ti alloys are poor thermal conductors, poor machinability due to hardening, strong tool wear, and burr formation characterize the micro-milling of these materials [32, 35]. According to Ahmadi et al. [124], the different grain sizes and phases located in the microstructure of Ti6Al4V in micro-milling affect the deformation behaviour of the material significantly. The smaller grain size and the smaller amount of β phase result in higher cutting forces within the alloy. In addition, it was found that the microstructure of the workpiece material also influences the size of the built-up edge: smaller grain size results in a larger built-up edge.

Table 2 summarises and categorises the workpiece materials, which were micro-machined in the reviewed key papers. We kept the standard used in the sources because in some cases, the permissible value of the alloy content differs in the different standards; thus, they cannot be perfectly matched to each other. Figure 9 shows the distribution of the reviewed scientific works from the point of view workpiece material groups.

2.9 Micro-milling process monitoring

The main purpose of process monitoring is to monitor changes of the cutting process and/or monitor the condition of the cutting tool in order to increase quality, efficiency or tool life [268]. Through its application, it is possible to prevent the changes with a negative effect. Process monitoring can be done online (in process) or offline, the former in real-time and the latter between cutting operations. Certain characteristics can be monitored in-process, such as cutting force, vibrations, power, torque, cutting temperature, and so on. Offline measurable parameters include tool wear, dimensional tolerance, surface roughness, delamination, micro-cracks etc.

As both process and quality characteristics are strongly influenced by tool wear, it is highly recommended to monitor it, which can be conducted based on the following two main measurement methods [269, 270]: (i) Direct measurement of tool wear: in this case, the wear of the tool can be measured directly (often optically). Its main disadvantage is that there is no cutting during the measurement (offline), which increases the total operation time. (ii) In the case of indirect measurement, the current state of the tool can be inferred from other process characteristics. In this case, the measurement of forces, vibrations, acoustic emissions [227] and the monitoring of their changes provide important information (indirect but online). In conventional-scale milling, tool wear has been studied in many studies, mainly using indirect measurement methods, like measuring vibration, acoustic emission, and force signals. Intelligent approaches can be used to process these data, such as neural networks and clustering [271, 272], adaptive resonance networks, and self-organising maps [227].

Zhu and Yu [27] presented a novel image processing based method for monitoring tool wear. It takes into account the wear pattern of the entire tool, through that it better reflects the condition of the tool than the traditional tool wear metrics, where only a width value is given. The current literature mainly uses the latter as a tool wear criterion. In the case of micro-milling, the wear of the cutting edges will often be different due to the different load. The effectiveness of the method presented by Zhu and Yu was also supported experimentally. Compared to other image processing methods, the presented technique reduces distortions caused by image background and noise.

According to Malekian et al. [273], accurate monitoring of machining typically requires three harmonic signals. In addition to the dynamometer's signal, it is advisable to use accelerometers and/or acoustic emission sensors due to the significantly larger frequency range available. In conventional-sized milling, the size of flank wear is measured usually. Due to the nature and difficult-to-measure wear in the case of micro-milling, the authors measured the corner radius. Neuro-Fuzzy logic was used to analyse the signals of the process, and it was found that the combined analysis of the signals of the three sensors leads to the most accurate result. The model presented by the authors is suitable for monitoring micro-milling tools and for transmitting warnings to the machine operator, thus minimising tool breakage and exceeding the tolerance of the part.

Zhu et al. [227] used the hidden Markov model to monitor the condition of the tool. The authors used the average clearance wear on each edge to rate the wear condition. The authors recommend the use of the Noisy-robust hidden Markov model to monitor the condition of the tool. The efficiency of their method is 92.5% in copper and 90.5% in steel.

Jemielniak and Arrazola [187] chose to measure clearance wear to monitor tool condition. Due to the varying load on the tool, the cutting forces must change periodically. If the tool run-out does not take into account, the dominant frequency will be the impact frequency of the cutting edges; otherwise, it will correspond to the spindle speed. When comparing the force signals and the acoustic emission (AE) signals, a difference in the dominant frequencies was found. The latter shows 1207 Hz, and the results of the force measurement show 4828 Hz, which is the fourth harmonic of the impact frequency of the edges, and it is close to the natural frequency of the force measuring platform (5080 Hz). According to the authors, the unfiltered, raw signal can also be used for monitoring applications, as the relationship between the characteristics of the

Table 2 Micro-milling publications categorized based on the machined material type

Material categories	Publications	
Steels	AISI 1045: [4], [33], [38], [46], [48], [51], [54], [83], [88], [89], [122], [133], [144], [164], [165], [166], [167], [168]	
	AISI 1015: [169]	S960QL: [171]
	AISI 1018: [125]	NAK80: [123], [172], [173], [174]
	AISI 1040: [77]	AISI A2—annealed: [175]
	AISI 1050: [37]	42CrMo4: [167]
	AISI 4340: [119], [139], [170]	X13NiMnCuAl4-2-1-1: [146]
	AISI P20: [20], [145], [164]	SK2: [176]
Hardened steels	AISI H13: [2], [30], [42], [72], [80], [164], [177], [178], [179], [180] Martensitic powder metallurgy steel: [84]	
	AISI A2: [175]	42NiCrMo16: [29]
	AISI D2: [181], [182], [183], [184]	55NiCrMoV6: [186]
	SKD 61: [147], [185]	X155CrVMo12-1: [187], [188], [189]
Corrosion resistance steels	AISI 304: [34], [106], [58], [190]	
	12Cr18Ni9: [43]	AISI 304L: [194]
	06Cr25Ni20: [191]	AISI 316L: [195], [49]
	90MnCrV8: [192]	AISI 422: [196]
	Stavax: [149]	X5CrNi1810: [197], [111], [114]
	Hastelloy C276: [193]	X2CrNi18-9: [198]
		Rochling 2316: [199]
Superalloys	Inconel 718: [41], [76], [85], [158], [159], [160], [196], [200], [201], [202]	
	Inconel 182: [203]	Nimonic 75: [79]
	GH4169: [204]	DD98: [205]
Titanium and its alloy	Ti-6Al-4V: [5], [32], [35], [70], [82], [86], [94], [108], [113], [124], [126], [129], [134], [150], [151], [152], [155], [156], [196], [206], [207], [208], [209], [210], [211], [212], [213], [214], [215], [216], [217]	
	Grade 2: [40], [193], [218], [219], [220]	TC4: [222]
	CP titanium: [221]	Grade 12: [223]
Copper and its alloys	Copper: [121], [224], [225], [226], [227]	
	OFC: [110], [120]	CuZn39Pb1: [102], [230]
	OFHC copper: [81], [91], [93], [228]	CuZn39Pb3: [167]
	Brass 360: [229]	CuZn40Pb2: [197]
	Brass260: [39]	Copper alloy: [231]
	CuZn37: [193]	Tungsten copper: [6], [128]
Aluminium alloys	Al 6061: [45], [78], [92], [109], [116], [117], [125], [148], [232], [233], [234], [235], [117], [236], [237], [238], [239] Al 7075: [36], [169], [240], [241], [242], [243], [244], [245]	
	Al 2024: [95], [246]	Al 7050: [142], [250]
	Al 2124: [58]	AA1100: [98]
	Al 6082: [77], [247], [248], [249]	AlCu4PbMgMn: [140]
	Al 6351: [3]	
Other materials	Monocrystalline silicon: [251], [252], [253], [254], [255]	
	Cemented carbide: [256], [257]	OFHC single-crystal: [228]
	WC-15Co: [258], [259]	Silicon: [264]
	Graphite: [260]	KDP crystal: [44], [101]
	LiNbO3: [261]	Sintered zirconia: [265]
	NiTi: [112]	ZrO2: [266]
	PMMA: [262], [263]	Glass: [267]
	QBe1.7: [115]	
	CFRP: [75]	

force signal and the wear is important and not their specific values. Uncertainties can be reduced and minimised by simultaneously recording and analysing the signals of multiple sensors. The use of these two sensors has led to good results. In contrast, the signal from the much cheaper, easy-to-install AE sensor produced less accurate but acceptable results.

One of the main problems of micro-milling is the premature failure of cutting tools. To predict tool life, Dai and Zhu [55] presented an automated machine vision system. In the captured images, the tool can be in any positions, and the algorithm can evaluate it correctly. This is based on the fact that the size of the tool (which perpendicular to the cutting edges of the tool) does

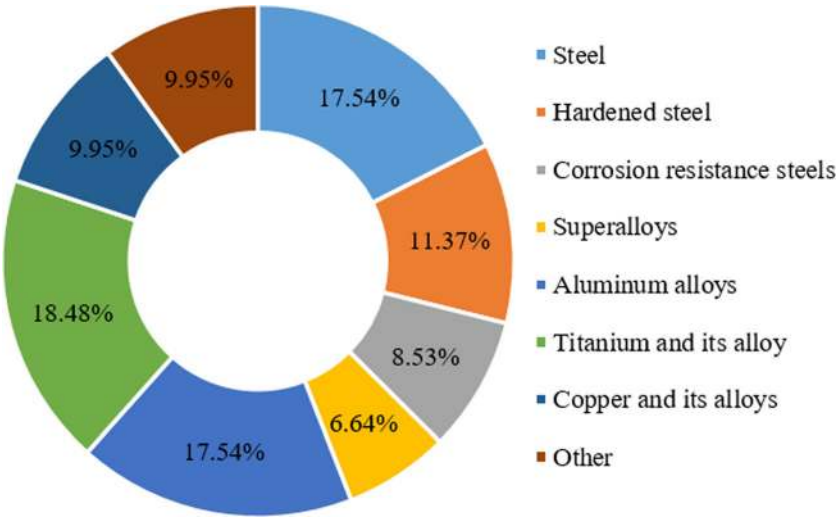

Fig. 9 Micro-milled workpiece material groups

not change. The image processing method is based on the characteristics of micro-milling, with the exception of the progressive wear phase. In order to predict the wear status of the tool, in addition to flank wear, a wear land area is recommended. When the tool arrived at the stage judged to be worn or experienced abnormal behaviour, they intervened in the process and reduced the feed. They highlighted that they did not encounter any accidental tool failure during their investigations.

Jáuregui et al. [54] dealt with tool monitoring through the analysis of force and vibration signals. Fast Fourier transformation and continuous wavelet transformation (CWT) were used for the investigations. The analysis of process-specific frequencies was based on the impact frequency of the cutting edges (*IPF*). For a tool in a good condition, the harmonic and non-harmonic components are displayed at the nominal frequency 1x*IPF*, 2x*IPF*, 3x*IPF* and 0.5x*IPF*, 1.5x*IPF*, 2.5x*IPF*. However, with a worn tool, those harmonic frequencies appear that are not exact fractions of the *IPF*. It was found that in the case of a tool in a good condition, the harmonic and non-harmonic frequencies are present at the nominal value, while in the case of a worn tool, the characteristic frequencies are different or missing. As the wear progressed, the appearance of new frequencies in the vibration signal was observed. FFTs made from force amplitudes did not provide any convincing evidence that they could be used as an indicator of tool wear. Similarly, the study of the effects at nonlinear levels by CWT analysis does not provide any evidence for a correlation of phenomena.

The main process control methods and monitored characteristics often used in micro-milling are summarised in Table 3.

3 Micro-milling tools and coatings

In this section, cutting tool geometries and coatings for micro-milling are reviewed and discussed. Micro-milling tools are geometrically similar to those used in conventional sizes, but often show different behaviour in terms of the cutting process. The key dimensions of the micro-cutting tools are often in the same order of magnitude as the key dimensions of the chip removal or burr formation processes, as it was discussed earlier. The micro-cutting tool is relatively slender, which often results in a difficult-to-estimate process, high vibrations and short tool life. Figure 10 summarises the micro-milling cutting tool types which are often used in scientific works or used by the industry.

End mills are widely used in micro sizes [4, 133, 144, 216], the geometry of which is similar to those used in macro-sizes. Commercially one- (Fig. 10a), two- (Fig. 10b) or multi-fluted versions are available. It is important to highlight that a higher number of cutting edges often drastically reduce the stiffness of the cutting tool, therefore, the lower number of cutting edges is recommended for micro-milling. Nevertheless, higher number of tool edges may increase the material removal rate (MMR) significantly. These type of the tools are suitable to produce structures with quasi-sharp corners. However, this geometry has many challenges: the corner starts to round relatively soon due to the wear, which results in significant changes in the tool geometry, in the process and in the produced microstructures. The single-fluted geometries are often made of artificial diamond [204, 255], which can result in a very sharp cutting edge; however, it often causes higher vibrations [109, 140].

Figure 10c shows a schematic of a micro flat end mill with a corner radius. Recently, this design is very common as it provides increased edge stability. The corner radius is much more resistant to wear compared to the previous designs. Furthermore, these milling tools can produce complex 3D curved surfaces. In addition, this construction can be used with increased feed rates in the case of smaller depth of cut values. In this scenario, the main cutting edge angle is smaller, which results in the chip thinning phenomena. Due to the

Table 3 Most important micro-milling monitoring methods and monitored parameters

Authors	Monitoring method	Monitored parameter
Jemielniak and Arrazola [187]	Acoustic emission measurement	Vibration
Malekian et al. [273]		
Jemielniak et al. [188]		
Ren et al. [189]		
Dai and Zhu [55]	Digital image processing	Tool wear
Zhu and Yu [27]		
Jáuregui et al. [54]	Acceleration measurement	Vibration
Malekian et al. [273]		
Hsieh et al. [176]		
Jáuregui et al. [54]	Piezoelectric-principle based force measurement	Cutting force
Jemielniak and Arrazola [187]		
Zhu et al. [227]		
Malekian et al. [273]		
Jemielniak et al. [188]		
Li and Liu [274]		
Venkata Rao [184]	Power or energy consumption measurement	Cutting force
Lu et al. [275]		
Peng et al. [191]	Thermocouple or infrared radiation measurement	Cutting temperature
Yang et al. [95]		

radius, there is an increased axial force component, which causes less bending-directional deformation in the tool than the cutting force, and also could be suitable to reduce the vibration [42].

Figure 10d shows the schematic of a ball-end micro mill, which is also commonly found in the scientific literature [174, 184, 255, 276]. This type is especially suitable to produce complex 3D geometries. However, it also has difficulties, e.g. when machining flat surfaces the cutting speed is very small near the tool centre point (TCP), and the minimum chip thickness problem comes to view due to the chip thinning phenomena. However, these difficulties can be solved partly with the use of push-milling or pull-milling strategies; although, it requires a more complex (4 or 5-axis) machining centre, which is extremely cost consuming.

The tapered micro-milling tools (Fig. 10e) are also applied widely, which is suitable to reduce the burr formation [109]. In addition, there are many papers, where tailored micro-tools are used for the optimisation of the process [108, 217].

According to Aramcharoen and Mativenga [72], the geometry of the cutting edge plays a major role in terms of surface quality and burr formation in micro-milling. For better surface quality, rounded cutting edges or chamfered geometries are preferred. Afazov et al. [119] studied the effect of the rake angle on AISI 4340 steel. Higher forces and lower stability limits were observed at rake angle of $\gamma = 0°$ than at $\gamma = 8°$. Based on the micro-milling studies in 42NiCrMo16, conducted by Gilbin et al. [29], it was found that the edge geometry of micro-mills has a greater role in wear resistance than in the quality of the machined part. In contrast to macro-milling, a rake angle of $\gamma = 0°$ is advantageous in decreasing tool wear, while its negative effect on the cutting forces is not significant. Based on the micro-milling experiments performed by Oliaeia and Karpat [149] in a modified AISI 420 steel, the interaction

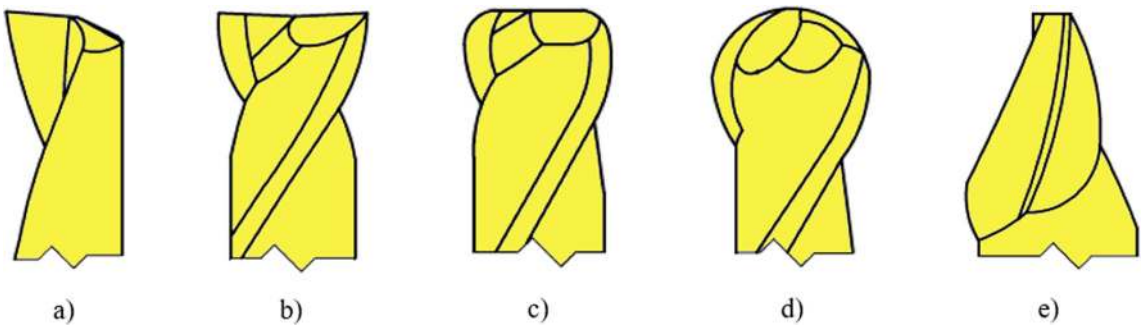

Fig. 10 Schematic geometries of micro-milling cutting tools: (a) single-fluted flat end mill, (b) two-fluted flat end mill (c) end mill with corner radius, (d) ball-end mill, (e) tapered micro mill

between the tool wear and the cutting speed is clearly visible, which is one of the main factors followed by feed per tooth. Tool wear is one of the most significant limitations of the micro-milling process, as it is almost unpredictable and also affects dimensions, surface quality, and tool life [192]. For this reason, the subject of many scientific researches is the examination of the geometry of milling tools and the increase of their performance. Uhlmann et al. [220] attached great importance to edge preparation in the production of micro-mills. Their studies were shown that immersed tumbling can achieve better results than polishing and polish blasting methods. Immersed tumbling on grade 2 titanium reduced active forces from 7.5 N to 4 N, while average surface roughness (R_a) increased to 0.67 μm from 0.53 μm. Tools prepared with this method were also tested in micro-machining of X13NiMnCuAl4-2-1-1. According to the authors, edge preparation can stabilise the cutting edge and reduce tool wear. Larger cutting edge radius led to longer tool life. The active forces were almost the same for the prepared and un-prepared tools, their fluctuation decreased to r_β = 2.9 μm, and then started to slightly increase [146]. The authors also studied tool wear on Böhler M261 material quality. During preparation, processing time was found to be the main factor in forming the cutting edge radius. No crater-wear-tendency was found for the geometries developed with the new method. The prepared tools showed a 14% lower tendency to clearance wear compared to the unprepared ones, while the variance of the results was reduced by 92% [87].

Micro cutting tools are often coated because coating has many positive effects on the machining process characteristics, like increasing tool life or reducing cutting force and vibrations. However, the application of coating increases the edge radius of the cutting tool, which is often not allowed because it may increase the ploughing effect and the cutting force, thus decreases tool life. Aramcharoen et al. [2] analysed the influences of different coatings on tool wear in a very fine-grained AISI H13. They showed that TiN, TiCN, TiAlN, CrN, and CrTiAlN coatings help to reduce edge chipping and increase edge rounding compared to uncoated ultrafine carbide milling cutter. The TiN and CrTiAlN coatings are suitable for reducing flank wear. Based on their studies, the TiN coating showed the best performance in terms of tool wear, machined surface and burr formation. Furthermore, TiN has the lowest hardness and the best adhesion. Aslantas et al. [94] analysed the tool wear of nanocrystalline diamond, TiN, AlCrN coated tools in Ti6Al4V. In their work, abrasive wear was found to be significant, and edge chipping and built-up edge formation were also observed. Each analysed coating reduced the resulting burr sizes compared to the uncoated tools. The TiN and AlCrN coatings showed less wear, diameter changes and burrs than it was observable by using a nanocrystalline diamond or an uncoated tool. De Cristofaro et al. [192] investigated seven different novel coatings (multilayer chromium, titanium coating, single-layer nanostructured silicon, chromium, and single-layer nanostructured coating with small, medium, and large amounts of silicon) in micro-milling of 1.2842 (62 HRC). The single-layer, nanostructured and low-silicon coating was found the best: this coating seemed to suitable for reducing wear while increasing productivity and reliability, as well as creating a sharp cutting edge. Swain et al. [79] performed micro-milling experiments on Nimonic 75 (40–41 HRC). They found that the typical failure modes of tool are the flank wear, the chipping of the tool tip and then chipping the edge. In the case of the 2 μm thick nanostructured TiAlN coating, the outstanding performance was observed in terms of wear, diameter reduction and surface integrity compared to the uncoated tool. It was found that the increase of the cutting speed resulted in an increase of the flank wear, in each coated and uncoated tools.

Hao et al. [257] designed and fabricated polycrystalline diamond (PCD) micro ball-end mills in order to achieve high quality when machining micro-lens array of cemented carbide. Since the diamond is very sensitive to the vibrations, the authors calculated the excitation frequency which related to the milling kinematics and to the number of the cutting edges. Moreover, modal analysis was conducted, and the natural frequencies (up to six order) were calculated. Based on their investigations, a critical overhanging length was determined for the specified cutting circumstances. Jiao and Cheng [263] used CVD diamond coated micro ball-end mills for micro-milling of polymethyl methacrylate components with a very small surface roughness (nanometric). Four different milling strategies were studied, and it was found that those ones, which are suitable for groove-milling, are not necessarily the best choice for preparing larger areas (2 x 2 mm) because the dynamics of the process also plays a significant role. When machining larger areas, optical surfaces can be achieved by joining up-milling and down-milling strategies. However, the step-over was found as the most significant factor that is affecting the surface roughness. Hao et al. [277] studied the fabrication methods for PCD micro-milling tools with a large aspect ratio. The authors proposed a fabrication method which is combined the pulsed nanosecond and picosecond laser with precision grinding. The micro tool fabricated was compared with a cemented carbide tool through micro-milling experiments. The PCD tool produced smaller surface roughness and forces, while the wear of the tool was smaller at machining a deep-narrow-slot in an oxygen-free copper. Oliaei and Karpat [108] investigated the formation of a predictable, stable built-up edge on Ti6Al4V. As this can increase the tool life, it can be especially important, when machining micro moulding tools. Based on their tests, the built-up edge resulted in higher cutting force and improved the surface quality. Based on their studies, the small clearance angle resulted in the most stable conditions in built-up edge formation, and based on their observations, the performance

of custom (tailored) tools is acceptable. Nevertheless, it has to be pointed out that a built-up edge formation is recommended to be avoided because it is extremely difficult to control its formation (to stabilise it) and influence.

Tool wear is primarily affected by tool edge geometry and coating type; however, the effect of primary technological parameters is also significant [180, 214]. Kuram and Ozcelik [35] investigated the effect of milling strategies on tool wear on TiAl4V6 material. At low feed rates (v_f = 75 mm/min), increasing the rotation speed (12,000–28,000 rpm) at the down-milling and zig-zag paths reduced tool wear, but the up-milling had a negative effect on the tool wear. At high feed rates (v_f = 150 mm/min), higher the spindle speed increased the tool wear for all the three strategies, resulting in better surface quality and smaller F_x and F_y forces. Up-milling is proposed in the case of low feed rates and high spindle speeds, and down-milling is more favourable in high feed and spindle speed. Oliaeia and Karpat [149] conducted pocket milling experiments on a Stavax stainless steel (25 HRC) with different cutting parameters. They found that the cutting speed has the most significant effect on tool wear, followed by the feed, depth of cut and cutting width, respectively. According to Aurich et al. [40], tilting the cutting tool may be advantageous, since in this case, the end of the tool is in a contact with only the bottom of the groove for a short length, which may result in reduced tool wear.

Chi-Hsiang et al. [185] investigated the micro-milling process using 2D finite element simulations on SKD61 material. Based on their simulation results, temperature and cutting force have the most significant effect on the condition of the cutting edge, which are important criteria for improving the performance of the tools. Based on their study, the rake angle has the largest effect on complex quality characteristics (37.80% contribution based on ANOVA), so it should be an important consideration in tool design. The optimal micro-milling design parameters were defined in γ = 20 °, α = 7 °, and the cutting parameters in v_c = 11.31 m/min and a_p = 0.01 mm. Under these conditions, the average cutting length of the tools was l_c = 299 mm.

4 Micro-milling modelling

Sufficiently accurate modelling of the micro-milling processes is of great importance because cutting force, cutting temperature, crack propagation, surface roughness, tool wear or tool breakage etc. can be estimated without numerous experimental work, which is often time and cost consuming. The micro-milling process was modelled and simulated by the researchers using (i) analytical models [78, 148, 239], (ii) numerical models [117, 191, 249], (iii) regression analysis [42, 171] or (iv) response surface methodology [200, 201, 205]. Table 4 summarises the key scientific studies from the past five years in the topic of modelling of the micro-milling process.

According to de Oliveira et al. [46], the behaviour of the specific cutting force at micro-sizes is much more sensitive to cutting conditions than the models set up by Taylor and Kienzle, which consider only the feed per tooth. The method proposed by the authors also takes the depth of cut into account. They also proved that the constants of macro-sized models cannot be directly adapted to micro-sizes. Biró and Szalay [171] extended the empirical specific cutting force model to the region of thin chip removal, and identified a new breakpoint in the region of the micro-chip removal.

Zhang et al. [148] presented a novel analytical cutting force model and a model estimating the instantaneous tool deformation. The run-out of the tool is taken into account, which includes differences originating form axial and tilt offset, the trochoidal trajectory and the different tool entry and exit angles. In addition, the size effect was also taken into consideration as a factor, with shear and ploughing dominant parts separated. During the validation of the results in Al6061-T6, a good agreement was found in a wide range of cutting parameters. The presented model is promising for monitoring the micro-milling process and for its adaptive control. In an advanced micro-milling force model, Afazov et al. [119] proposed to consider tool run-out, edge radius, cutting speed, tool helix and rake angle, and workpiece preheating.

Numerical modelling is becoming increasingly important as modern computers allow increasingly complex simulations to be performed at significantly lower costs compared to experimental methods. Jin and Altinas [39] estimated the cutting forces of micro-milling on Brass 260 material using a finite element method. Cutting coefficients were taken into account in the milling model, which includes helix angle, tool trajectory, tool run-out, and the dynamics of the dynamometer. Based on their results, the estimation of normal directional cutting forces is accurate, but the feed forces are less reliable due to the friction model built into the finite element model. If the friction model can be improved, the estimation accuracy of the feed forces can be close to the results of the slip-line model. Lu et al. [76] presented a 3D coupled thermo-mechanical cutting force model that takes the effect of tool flank wear into account in nickel-based superalloys. Wear was studied using a finite element model, which was found to be an effective method. The model is based on their three-dimensional, dynamic cutting force estimator analytical model presented earlier [202], which also took size effects, elastic recovery, and tool run-out into account.

The force model presented by Mamedov et al. [142] calculates the actual chip thickness, which considers the trajectory of the tool as it rotates and translates. In addition, the model takes into account the ploughing force and the elastic recovery of the material. The tool deformations may result in the imperfection of the produced part; therefore, the monitoring or

Table 4 Scientific studies in the modelling of the micro-milling process

Authors	Type of modelling	Input variables	Response variables
Zhang et al. [148]	Analytical modelling	Run-out, trochoidal trajectory, tool deflection	Cutting forces Instantaneous tool deformation
Biró and Szalay [171]	Regression analysis	Cutting speed, feed rate, depth of cut, and milling strategy	Specific cutting force
Jing et al. [216]	Mechanic model, FEM	h_{min}, run-out, elastic recovery of the material, variety of entry and exit angles of the flutes	Cutting force, instantaneous uncut chip thickness
Zhang et al. [239]	Analytical modelling	Stochastic tool wear, run-out, trajectory of cutting edge, h_{min}, elastic recovery	Surface topography, surface roughness
Zhang et al. [78]	Analytical modelling	h_{min}, size effect	Burr formation (Poisson and exit burr size)
Davoudinejad et al. [249]	Finite element modelling	Spindle speed, depth of cut	Thin features
Chen et al. [168]	Finite element modelling	h_{min}, tool run-out	Surface profile, surface roughness
Peng et al. [191]	Finite element modelling	Cutting speed, feed rate	Temperature and cutting deformation
Wojciechowski et al. [47]	Combined numerical-analytical approach	Geometric errors of the machining system, tool deformation, minimum UCT, chip thickness accumulation	Cutting force
Yuan et al. [117]	Finite element modelling	UCT, exact trochoidal trajectory of tool tip, run-out, h_{min}, elastic recovery, variation entry and exit angles Strain hardening, strain rate sensitivity, thermal softening behaviour, and temperature-dependency	Cutting force
Yadav et al. [215]	Finite element modelling	Cutting speed	Exit burr size on the up-milling side
Balázs and Takács [42]	Regression analysis	Chip-cross-section, contact length between the workpiece and cutting edge	Cutting force
Gao et al. [205]	Molecular dynamics	Cutting speed, feed rate, depth of cut	Average surface roughness, easy slip line, slip behaviour of the lattice
Lu et al. [200]	Response surface methodology	Spindle speed, feed per tooth, depth of cut	Vickers hardness
Lu et al. [201]	Response surface methodology	Spindle speed, feed per tooth, depth of cut	Surface roughness
Gao et al. [205]	Response surface methodology	Spindle speed, feed per tooth, depth of cut	Surface roughness
Abolfazl Zahedi et al. [278]	Smoother particle hydrodynamics combined with continuum finite element analysis	Crystal orientation	Cutting force, chip morphology

estimating tool deformations is recommended by the researchers. The presented model was validated by micro-milling experiments on Al 7075. According to Li et al. [225], it is difficult to accurately model the current theoretical-chip thickness due to the run-out of the tool and single-edge-cutting phenomenon. A generic instantaneous undeformed chip thickness model has been presented that takes into account the difficulties mentioned above. In this model, the trajectory of the tool is taken into account for a complete cycle. The presented model is much more accurate than the previous ones, according to the authors. Jun et al. [143] have also developed a chip thickness model for micro-milling that takes into account the minimum chip thickness, the elastic recovery, and the elastic-plastic nature of the workpiece. The authors also presented a cutting force model that shows the effect of the size of the stable built-up-edge and the special cutting mechanism of micro-milling caused by the edge radius and the effective rake angle. The approach of the slip-line plasticity model also takes into account the chip separation and the ploughing/rubbing phenomenon, caused by the minimum chip thickness during micro-milling.

Niu et al. [248] investigated the process of chip formation on Al6082 using an analytical model. Based on their research results, in the case of carbide tools, the chips formed in successive turns are affected by the tool/workpiece material pairing (affected by the tool/material interfacial pair) and the tool radius, while in the case of a perfectly sharp diamond tool, the chips are more separated and remained intact. The finite element model developed by Chi-Hsiang et al. [185] treats the tool's operating rake angle, clearance angle, cutting speed, and depth of cut as factors. Their model can be a strong reference for tool manufacturers to design the geometric angles of micro-milling tools, and the micro-machining process. Wang et al. [41] developed a model of a micro-milling process based on finite element simulations on Inconel 718. It has been found that by increasing the feed and depth of cut, the presence of continuous chip removal becomes much more apparent while the forces also increase. Zhou et al. [123]

investigated the cutting forces of micro-milling through finite element simulation of orthogonal chip separation in NAK80 steel. The model includes the tool trajectory, run-out, edge radius, rake angle, the relationship between the workpiece and the tool, and the mechanical and physical properties of the material. Based on their simulations, in the range of the parameters of v_c = 12–36 m/min, f_z = 0.3–12 μm, the highest Von Mises stress in the secondary shear zone was 2000 MPa.

Mamedov and Lazoglu [126] investigated the cutting temperature in the primary and secondary deformation zones by finite element modelling in Ti6Al4V. In their model, the temperatures of the tool and the workpiece are estimated using analytically estimated shear and frictional heat output. The model was validated by experiments, where the results showed a match within 12%. Yang et al. [95] investigated the temperature distribution for Al2024-T6 micro-machining using a new thermomechanical model. It was found that with increasing tool radius (0; 3.2; 5; 7 μm) the temperature of the tool decreases (57.5; 51.5; 45.4; 40.4 ° C, respectively). These values are low compared to conventional sized milling. In addition, the cutting forces increased, but effective stress showed a decrease. Wissmiller and Pfefferkorn [125] studied the temperature distribution of micro-mills with a 2D, axially symmetric, transient finite element modelling in order to develop a strategy that potentially improves tool life and machining accuracy through temperature distribution. The modelling showed a good agreement with the experiments, using the carefully chosen heat input, the results were more favourable for steel than for aluminium. Shorter cutting edges and a shorter transition section are recommended due to the lower thermal resistance, as it allows faster heat flow, thereby further reducing the tool temperature.

Beruvides et al. [6] proposed the real-time monitoring of vibrations, based on a neuro-fuzzy model to estimate the roughness of micro-machined surfaces. Their method estimates the surface quality with an error of 9.5%. Afazov et al. [139] presented a novel vibration model (chatter) that includes the nonlinearity of uncut chip thickness, including tool run-out as well as tool-holder-spindle dynamics. According to the authors, the nonlinearity of the cutting force is mainly caused by the (i) run-out of the tool, (ii) edge radius and (iii) cutting speed. As the tool run-out increases, the stability curves shift in the direction of the cutting speed axis, and the stability range decreases.

Abolfazl Zahedi et al. [272] presented a hybrid method which combines the smoother particle hydrodynamics (SPH) with the continuum finite element analysis. The SPH is a mesh-free method, which is advantageous in the cutting zone where the strain and the strain-rate are high, while the continuum finite element model is advantageous for the rest of the workpiece in order to reduce the computational time. In their study, the effect of different crystal orientations (single crystal copper) on the cutting force and the chip morphology was analysed. It was found that the cutting force is the most sensitive in the direction of (101). Taking into consideration all of the evaluated crystal orientation, the difference in the cutting force was 33%. The chip morphology was found different in every orientation. Moreover, the results were verified by orthogonal cutting experiments.

The molecular dynamic is a widely used simulation method due to its special circumstances. The method based on the solving of Newton's movement equations, and it describes the interactions of the particles in the atomic level [279]. There are many papers in the case of nano-scale machining [279–282]; however, its application is very limited in the studies, which aim the investigation of the macro or micro-milling processes. Xiao et al. [283] investigated the transition mechanism from brittle to ductile mode at machining brittle material (6H SiC) with molecular dynamics method. It was found that the brittle mode machining can be achieved by the increased undeformed chip thickness. Based on their study, (i) at 40 nm undeformed chip thickness, the brittle fractures dominates the material removal, while (ii) at h = 30–35 nm both the brittle fracture and ductile chip formation occur. (iii) If the value of h is under 25 nm the dominant mechanism is the ductile chip removal. These simulations were verified by the authors with plunge experiments.

5 Future trends and outlook

As it was highlighted in the introduction, the miniaturisation is a well-established recent demand of the industrial sectors, highly encouraged by the recommendations and laws of national governments and by the European Union [1]; therefore, current micro-milling technologies are widely investigated and applied [284]. Nevertheless, there are still many novel trends and challenges, which have to be worked on in the future. Although current micro-milling technologies are often able to generate high-quality micro-features in several materials, it is highly encouraged: to increase (i) material removal rate, (ii) tool life, (iii) cost-effectiveness, (iv) flexibility; and decrease (v) operation time, (vi) burr formation and (vii) surface roughness. These issues could be partly improved by using the following processes: hybrid micro-milling technologies, green or sustainable micro-milling, smart micro-milling or artificial intelligence controlled technologies.

Hybrid micro-milling technologies try to fuse the advantages of the mechanical micro-milling and another advanced technology to—more or less—increase (i)–(iv) or decrease (v)–(vii) properties of the process [285]. Ultrasonic vibration-assisted micro-machining is a promising novel technology, which is able to decrease the cutting force, burr formation and surface roughness, compared to the mechanical micro-milling [236, 286–288]. Furthermore, the wettability of the micro-machined surfaces can be more advantageous, if the cutting tool or the workpiece is vibrated in an optimised

ultrasonic frequency. The tool life and the process efficiency can be increased by the application of laser supported micro-machining technologies [195, 196, 289, 290]. Their application also helps to improve the surface quality. With due regard to the thermal effects, burr formation can be reduced for difficult-to-cut materials like titanium alloys or composites [68, 291]. The cutting forces can be significantly reduced and it can also be used to process special or brittle materials (e.g. borosilicate glass). The focused ion beam micro-machining is also a promising technology, which is able to generate high-quality micro-features in difficult-to-cut materials, e.g. an extremely low average surface roughness (R_a = 5.6 nm) could be achieved in polycrystalline materials [256]. Moreover, the micro-milling of soft materials could also be fairly complicated; however, the ball burnishing technology [292] can be applied in order to increase the hardness of the upper surface, which can result in better cutting conditions.

Micro-milling accuracy depends significantly on the key elements of the machine tool (e.g. spindle, motion axes) [293, 294]. According to Luo et al. [295], bench-type ultra-precision machines will be one of the future development tendencies. They also highlighted that further investigation is needed to optimise and develop micro-milling tooling fabrication, fixturing and tool condition monitoring methods.

Green or sustainable micro-milling is going to probably spread more and more due to the increasing attention to the environment, although it is often a difficult-to-apply or costly technology [184, 296]. Furthermore, the energy-consumption minimisation and the refusal of use of application of cutting fluids (dry machining) often conflict with operation time minimisation or efficiently. In addition to dry machining, minimum quantity lubrication is becoming more widespread [160, 203] and special (e.g. nanofluid) and hybrid cooling lubrication systems have also appeared [152, 156, 297], and their use is expected to increase.

Smart micro-milling or artificial intelligence controlled technologies tries to minimise operation time, maximise material removal rate and increase tool life by the application of process monitoring and diagnostics. In the future, more industry 4.0 solutions (big data, artificial neural networks, neuro-fuzzy systems, cloud processing, digital twin etc.) will be probably implemented into micro-milling processes [227, 298–300]. Not only the process smartening but also the cutting tool smartening will be probably the scope of the near-future, e.g. realise bio-inspired tool self-sharpening or tool self-healing [301].

6 Conclusions

In the present paper, current studies dealing with micro-milling technologies were reviewed with particular attention to the discussion of the influences of the process parameters on the cutting force, temperature, vibration and surface roughness. Based on the present review, the following conclusions can be drawn:

- Micro-milling is suitable for producing complex 3D geometries in several materials; however, its application still meets many challenges and difficulties: (i) the tool wear often result in not only inappropriate machined surfaces but also in tool breakage; (ii) it is a difficult-to-predict process due to the size effect, ploughing effect and microstructure (e.g. inhomogeneity, material defects) of the workpiece; (iii) it is challenging to remove micro-machining induced burr; (iv) inappropriate vibration often breaks the cutting tool; (v) it is a difficult-to-monitor process due to the relatively small forces and measures.
- Chip removal and burr formation mechanisms of micro-milling significantly differ from the mechanisms known in macro-sized machining if the size of the theoretical chip thickness is comparable to the size of the minimum chip thickness. The ploughing effect often dominates the process, and the shearing mechanism is only secondary.
- The cutting force, cutting temperature and vibrations in micro-milling of quasi-homogeneous materials can be precisely estimated by experimental or theoretical models. However, it is still difficult to estimate these parameters if not only the micro-structure of the workpiece is inhomogeneous, but the macrostructure also (e.g. composites or sandwich structures), and if the machined geometry is complex (needs 4 or 5 axis movements).
- Both process and quality characteristics are strongly influenced by tool wear in micro-milling, it is therefore highly recommended to monitor it, which can be conducted based on direct measurement (often optically), or indirect measurement (cutting forces, vibrations, cutting temperature, power etc.) methods. Monitoring and diagnostics of the micro-milling process are extremely challenging because the values of monitored parameters are often too small and difficult to measure.
- Although current micro-milling technologies are often able to generate high-quality micro-features in several materials, it is highly encouraged to increase material removal rate, tool life, cost-effectiveness, and flexibility; and decrease operation time, burr formation and surface roughness. These issues could be partly improved by using hybrid micro-milling technologies, green or sustainable micro-milling, smart micro-milling or artificial intelligence controlled technologies.

Acknowledgements The research reported in this paper and carried out at BME has been partly supported by the NRDI Fund (TKP2020 NC, Grant No. BME-NC) based on the charter of bolster issued by the NRDI Office under the auspices of the Ministry for Innovation and Technology. This research was partly supported by the National Research, Development

and Innovation Office (NKFIH) No. OTKA-PD20-134430, OTKA-K-132430, and ÚNKP-20-3.

Authors' contributions (according to the CRediT taxonomy)
Barnabás Zoltán Balázs: conceptualization; writing–original draft preparation; visualisation; project administration
Norbert Geier: writing–original draft preparation; visualisation
Márton Takács: writing–review and editing; supervision
J Paulo Davim: writing–review and editing, supervision

Funding Open Access funding provided by Budapest University of Technology and Economics.

Compliance with ethical standards

Competing interests Not applicable

Ethical approval Not applicable

Consent to participate Not applicable

Consent to publish Not applicable

References

1. Missions in Horizon Europe | European Commission. https://ec.europa.eu/info/horizon-europe-next-research-and-innovation-framework-programme/missions-horizon-europe_en. Accessed 16 Mar 2020
2. Aramcharoen A, Mativenga PT, Yang S et al (2008) Evaluation and selection of hard coatings for micro milling of hardened tool steel. Int J Mach Tools Manuf 48:1578–1584. https://doi.org/10.1016/j.ijmachtools.2008.05.011
3. Moges TM, Desai KA, Rao PVM (2016) Improved process geometry model with cutter runout and elastic recovery in micro-end milling. Procedia Manuf 5:478–494. https://doi.org/10.1016/j.promfg.2016.08.040
4. Balázs BZ, Szalay T, Takács M (2017) Investigation of micro milled surface characteristics. Proceedings of International Conference on Innovative Technologies 161–164
5. Mittal RK, Kulkarni SS, Singh RK (2017) Effect of lubrication on machining response and dynamic instability in high-speed micromilling of Ti-6Al-4V. J Manuf Process 28:413–421. https://doi.org/10.1016/j.jmapro.2017.04.007
6. Beruvides G, Castaño F, Quiza R, Haber RE (2016) Surface roughness modeling and optimization of tungsten–copper alloys in micro-milling processes. Measurement 86:246–252. https://doi.org/10.1016/j.measurement.2016.03.002
7. Wang K, Zhang Q, Zhang J (2019) Evaluation of scale effect of micro electrical discharge machining system. J Manuf Process 38:174–178. https://doi.org/10.1016/j.jmapro.2019.01.005
8. Kim Y-S, Chu C-N (2018) The effects of graphite powder on tool wear in micro electrical discharge machining. Procedia CIRP 68:553–558. https://doi.org/10.1016/j.procir.2017.12.121
9. Kuzin VV, Fedorov SY, Szalay T, Farkas B (2016) Micromachining of a high-density current-conducting ceramic with the use of electrical-discharge Machining. Part 1. Refract Ind Ceram 57:164–169. https://doi.org/10.1007/s11148-016-9948-z
10. Kuzin VV, Fedorov SY, Szalay T, Farkas B (2016) Micromachining of a high-density current-conducting ceramic with the use of electrical-discharge machining. Part 2. Refract Ind Ceram 57:283–287. https://doi.org/10.1007/s11148-016-9969-7
11. Weng F, Liu Y, Chew Y et al (2020) IN100 Ni-based superalloy fabricated by micro-laser aided additive manufacturing: correlation of the microstructure and fracture mechanism. Mater Sci Eng: A:139467. https://doi.org/10.1016/j.msea.2020.139467
12. Allegre OJ, Li Z, Li L (2019) Tailored laser vector fields for high-precision micro-manufacturing. CIRP Ann 68:193–196. https://doi.org/10.1016/j.cirp.2019.04.125
13. Cadot GBJ, Axinte DA, Billingham J (2016) Continuous trench, pulsed laser ablation for micro-machining applications. Int J Mach Tools Manuf 107:8–20. https://doi.org/10.1016/j.ijmachtools.2016.04.011
14. Derevyanko DI, Shelkovnikov VV, Orlova NA et al (2017) Fabrication of high-aspect-ratio microstructures for LIGA-technology by sinchrotron radiation polymerisation of thetetraacrylate monomer. Phys Procedia 86:122–126. https://doi.org/10.1016/j.phpro.2017.01.032
15. Ma Y, Liu W, Liu C (2019) Research on the process of fabricating a multi-layer metal micro-structure based on UV-LIGA overlay technology. Nanotechnol Precis Eng 2:83–88. https://doi.org/10.1016/j.npe.2019.07.002
16. Silvestre CM, Nguyen V, Jansen H, Hansen O (2020) Deep reactive ion etching of 'grass-free' widely-spaced periodic 2D arrays, using sacrificial structures. Microelectron Eng 223:111228. https://doi.org/10.1016/j.mee.2020.111228
17. Li Y, Zhang H, Yang R et al (2019) In-plane silicon microneedles with open capillary microfluidic networks by deep reactive ion etching and sacrificial layer based sharpening. Sensors Actuators A Phys 292:149–157. https://doi.org/10.1016/j.sna.2019.04.008
18. Hamdana G, Puranto P, Langfahl-Klabes J et al (2018) Nanoindentation of crystalline silicon pillars fabricated by soft UV nanoimprint lithography and cryogenic deep reactive ion etching. Sensors Actuators A Phys 283:65–78. https://doi.org/10.1016/j.sna.2018.09.035
19. Bogaerts W, Dumon P, Taillaert D et al (2004) SOI nanophotonic waveguide structures fabricated with deep UV lithography. Photonics Nanostruct Fundam Appl 2:81–86. https://doi.org/10.1016/j.photonics.2004.07.002
20. Sahoo P, Patra K, Szalay T, Dyakonov AA (2020) Determination of minimum uncut chip thickness and size effects in micro-milling of P-20 die steel using surface quality and process signal parameters. Int J Adv Manuf Technol 106:4675–4691. https://doi.org/10.1007/s00170-020-04926-6
21. Ren Y, Li C, Li W et al (2019) Study on micro-grinding quality in micro-grinding tool for single crystal silicon. J Manuf Process 42:246–256. https://doi.org/10.1016/j.jmapro.2019.04.030
22. Leo Kumar SP (2019) Measurement and uncertainty analysis of surface roughness and material removal rate in micro turning operation and process parameters optimization. Measurement 140:538–547. https://doi.org/10.1016/j.measurement.2019.04.029

23. Suresh N, Ganesh S, Jagadesh T (2020) Investigations into edge radius and point angle on energy consumption during micro drilling of titanium alloy. Mater Today: Proc. https://doi.org/10.1016/j.matpr.2019.12.167
24. Liao Z, Axinte DA (2016) On monitoring chip formation, penetration depth and cutting malfunctions in bone micro-drilling via acoustic emission. J Mater Process Technol 229:82–93. https://doi.org/10.1016/j.jmatprotec.2015.09.016
25. Bissacco G, Hansen HN, De Chiffre L (2005) Micromilling of hardened tool steel for mould making applications. J Mater Process Technol 167:201–207. https://doi.org/10.1016/j.jmatprotec.2005.05.029
26. Alting L, Kimura F, Hansen HN, Bissacco G (2003) Micro engineering. CIRP Ann 52:635–657. https://doi.org/10.1016/S0007-8506(07)60208-X
27. Zhu K, Yu X (2017) The monitoring of micro milling tool wear conditions by wear area estimation. Mech Syst Signal Process 93:80–91. https://doi.org/10.1016/j.ymssp.2017.02.004
28. Chae J, Park SS, Freiheit T (2006) Investigation of micro-cutting operations. Int J Mach Tools Manuf 46:313–332. https://doi.org/10.1016/j.ijmachtools.2005.05.015
29. Gilbin A, Fontaine M, Michel G et al (2013) Capability of tungsten carbide micro-mills to machine hardened tool steel. Int J Precis Eng Manuf 14:23–28. https://doi.org/10.1007/s12541-013-0004-3
30. Lauro CH, Brandão LC, Filho SLMR, Baldo D (2014) Analysis of the forces in micromilling of hardened AISI H13 steel with different grain sizes using the Taguchi methodology. Adv Mech Eng 6:465178. https://doi.org/10.1155/2014/465178
31. Masuzawa T, Tönshoff HK (1997) Three-dimensional micromachining by machine tools. CIRP Ann Manuf Technol 46:621–628. https://doi.org/10.1016/S0007-8506(07)60882-8
32. Kumar P, Bajpai V, Singh R Burr height prediction of Ti6Al4V in high speed micro-milling by mathematical modeling. Manuf Lett. https://doi.org/10.1016/j.mfglet.2016.10.001
33. Jin X, Altintas Y (2013) Chatter stability model of micro-milling with process damping. J Manuf Sci Eng 135:031011-031011–9. https://doi.org/10.1115/1.4024038
34. Kuram E, Ozcelik B (2016) Micro-milling performance of AISI 304 stainless steel using Taguchi method and fuzzy logic modelling. J Intell Manuf 27:817–830. https://doi.org/10.1007/s10845-014-0916-5
35. Kuram E, Ozcelik B (2016) Effects of tool paths and machining parameters on the performance in micro-milling of Ti6Al4V titanium with high-speed spindle attachment. Int J Adv Manuf Technol 84:691–703. https://doi.org/10.1007/s00170-015-7741-7
36. Sun Q, Cheng X, Liu Y et al (2017) Modeling and simulation for micromilling mechanisms. Procedia Eng 174:760–766. https://doi.org/10.1016/j.proeng.2017.01.219
37. Yılmaz EE, Budak E, Özgüven HN (2016) Modeling and measurement of micro end mill dynamics using inverse stability approach. Procedia CIRP 46:242–245. https://doi.org/10.1016/j.procir.2016.04.114
38. Takács M, Balázs BZ, Jáuregui JC (2017) Dynamical aspects of micro milling process. Proceedings of International Conference on Innovative Technologies 181–184
39. Jin X, Altintas Y (2012) Prediction of micro-milling forces with finite element method. J Mater Process Technol 212:542–552. https://doi.org/10.1016/j.jmatprotec.2011.05.020
40. Aurich JC, Bohley M, Reichenbach IG, Kirsch B (2017) Surface quality in micro milling: influences of spindle and cutting parameters. CIRP Ann 66:101–104. https://doi.org/10.1016/j.cirp.2017.04.029
41. Wang F, Cheng X, Liu Y et al (2017) Micromilling simulation for the hard-to-cut material. Procedia Eng 174:693–699. https://doi.org/10.1016/j.proeng.2017.01.209
42. Balázs BZ, Takács M (2020) Experimental investigation and optimisation of the micro milling process of hardened hot-work tool steel. Int J Adv Manuf Technol. https://doi.org/10.1007/s00170-020-04991-x
43. Gao S, Pang S, Jiao L et al (2017) Research on specific cutting energy and parameter optimization in micro-milling of heat-resistant stainless steel. Int J Adv Manuf Technol 89:191–205. https://doi.org/10.1007/s00170-016-9062-x
44. Chen N, Li L, Wu J et al (2019) Research on the ploughing force in micro milling of soft-brittle crystals. Int J Mech Sci 155:315–322. https://doi.org/10.1016/j.ijmecsci.2019.03.004
45. Dib MHM, Duduch JG, Jasinevicius RG (2018) Minimum chip thickness determination by means of cutting force signal in micro endmilling. Precis Eng 51:244–262. https://doi.org/10.1016/j.precisioneng.2017.08.016
46. de Oliveira FB, Rodrigues AR, Coelho RT, de Souza AF (2015) Size effect and minimum chip thickness in micromilling. Int J Mach Tools Manuf 89:39–54. https://doi.org/10.1016/j.ijmachtools.2014.11.001
47. Wojciechowski S, Matuszak M, Powałka B et al (2019) Prediction of cutting forces during micro end milling considering chip thickness accumulation. Int J Mach Tools Manuf 147:103466. https://doi.org/10.1016/j.ijmachtools.2019.103466
48. Takács M, Verő B (2007) Actual feed rate per tooth at micro milling. Mater Sci Forum 537–538:695–700. https://doi.org/10.4028/www.scientific.net/MSF.537-538.695
49. Hajiahmadi S (2019) Burr size investigation in micro milling of stainless steel 316 L. Int J Lightweight Mater Manuf 2:296–304. https://doi.org/10.1016/j.ijlmm.2019.07.004
50. Yang Y, Han J, Hao X et al (2020) Investigation on micro-milling of micro-grooves with high aspect ratio and laser deburring. Proc Inst Mech Eng B J Eng Manuf 234:871–880. https://doi.org/10.1177/0954405419893491
51. Zhang T, Liu Z, Xu C (2013) Influence of size effect on burr formation in micro cutting. Int J Adv Manuf Technol 68:1911–1917. https://doi.org/10.1007/s00170-013-4801-8
52. Wang Y, Zou B, Yin G (2019) Wear mechanisms of Ti(C7N3)-based cermet micro-drill and machining quality during ultra-high speed micro-drilling multi-layered PCB consisting of copper foil and glass fiber reinforced plastics. Ceram Int 45:24578–24593. https://doi.org/10.1016/j.ceramint.2019.08.187
53. MICROMASTER® 3/5X - KUGLER GmbH. https://www.kugler-precision.com/index.php?MICROMASTER%2D%2D3-5X-EN. Accessed 15 May 2020
54. Jáuregui JC, Reséndiz JR, Thenozhi S et al (2018) Frequency and time-frequency analysis of cutting force and vibration signals for tool condition monitoring. IEEE Access PP:1–1. https://doi.org/10.1109/ACCESS.2018.2797003
55. Dai Y, Zhu K (2017) A machine vision system for micro-milling tool condition monitoring. Precis Eng. https://doi.org/10.1016/j.precisioneng.2017.12.006
56. Miao JC, Chen GL, Lai XM et al (2007) Review of dynamic issues in micro-end-milling. Int J Adv Manuf Technol 31:897–904. https://doi.org/10.1007/s00170-005-0276-6
57. Boswell B, Islam MN, Davies IJ (2018) A review of micro-mechanical cutting. Int J Adv Manuf Technol 94:789–806. https://doi.org/10.1007/s00170-017-0912-y
58. Lekkala R, Bajpai V, Singh RK, Joshi SS (2011) Characterization and modeling of burr formation in micro-end milling. Precis Eng 35:625–637. https://doi.org/10.1016/j.precisioneng.2011.04.007
59. Câmara MA, Rubio JCC, Abrão AM, Davim JP (2012) State of the art on micromilling of materials, a review. J Mater Sci Technol 28:673–685. https://doi.org/10.1016/S1005-0302(12)60115-7
60. Anand RS, Patra K (2014) Modeling and simulation of mechanical micro-machining—a review. Mach Sci Technol 18:323–347. https://doi.org/10.1080/10910344.2014.925377

61. Cardoso P, Davim JP (2012) A brief review on micromachining of materials
62. Liu J, Li J, Xu C (2014) Interaction of the cutting tools and the ceramic-reinforced metal matrix composites during micro-machining: a review. CIRP J Manuf Sci Technol 7:55–70. https://doi.org/10.1016/j.cirpj.2014.01.003
63. Robinson GM, Jackson MJ (2005) A review of micro and nanomachining from a materials perspective. J Mater Process Technol 167:316–337. https://doi.org/10.1016/j.jmatprotec.2005.06.016
64. Cardoso P, Davim JP (2012) Micro milling of metallic materials-a brief overview. Trans FAMENA 36:79–85
65. Póka G, Németh I (2020) The effect of radial rake angle on chip thickness in the case of face milling. Proc Inst Mech Eng B J Eng Manuf 234:40–51. https://doi.org/10.1177/0954405419849245
66. Samuel J, Jun MBG, Ozdoganlar B et al Micro/meso-scale mechanical machining 2020: a two decade state-of-the-field review. J Manuf Sci Eng:1–35. https://doi.org/10.1115/1.4047621
67. Bai W, Sun R, Roy A, Silberschmidt VV (2017) Improved analytical prediction of chip formation in orthogonal cutting of titanium alloy Ti6Al4V. Int J Mech Sci 133:357–367. https://doi.org/10.1016/j.ijmecsci.2017.08.054
68. Geier N, Davim JP, Szalay T (2019) Advanced cutting tools and technologies for drilling carbon fibre reinforced polymer (CFRP) composites: a review. Compos A: Appl Sci Manuf 125:105552. https://doi.org/10.1016/j.compositesa.2019.105552
69. Pereszlai C, Geier N (2020) Comparative analysis of wobble milling, helical milling and conventional drilling of CFRPs. Int J Adv Manuf Technol. https://doi.org/10.1007/s00170-019-04842-4
70. Vipindas K, Anand KN, Mathew J (2018) Effect of cutting edge radius on micro end milling: force analysis, surface roughness, and chip formation. Int J Adv Manuf Technol 97:711–722. https://doi.org/10.1007/s00170-018-1877-1
71. Klocke F (2011) Manufacturing processes 1 cutting. Springer-Verlag, Berlin Heidelberg
72. Aramcharoen A, Mativenga PT (2009) Size effect and tool geometry in micromilling of tool steel. Precis Eng 33:402–407. https://doi.org/10.1016/j.precisioneng.2008.11.002
73. Trent EM, Wright PK (2000) Metal cutting, 4th edn. Butterworth–Heinemann
74. Takács M (2006) Sokkristályos ötvözetek mikroforgácsolása keményfém szármaróval, Dissertation, Budapest University of Technology and Economics
75. Anand RS, Patra K (2017) Mechanistic cutting force modelling for micro-drilling of CFRP composite laminates. CIRP J Manuf Sci Technol 16:55–63. https://doi.org/10.1016/j.cirpj.2016.07.002
76. Lu X, Wang F, Jia Z et al (2017) A modified analytical cutting force prediction model under the tool flank wear effect in micro-milling nickel-based superalloy. Int J Adv Manuf Technol:1–8. https://doi.org/10.1007/s00170-017-0001-2
77. Liu X, DeVor RE, Kapoor SG (2005) An analytical model for the prediction of minimum chip thickness in micromachining. J Manuf Sci Eng 128:474–481. https://doi.org/10.1115/1.2162905
78. Zhang X, Yu T, Wang W, Zhao J (2019) Improved analytical prediction of burr formation in micro end milling. Int J Mech Sci 151:461–470. https://doi.org/10.1016/j.ijmecsci.2018.12.005
79. Swain N, Venkatesh V, Kumar P et al (2017) An experimental investigation on the machining characteristics of Nimonic 75 using uncoated and TiAlN coated tungsten carbide micro-end mills. CIRP J Manuf Sci Technol 16:34–42. https://doi.org/10.1016/j.cirpj.2016.07.005
80. Afazov SM, Ratchev SM, Segal J (2012) Prediction and experimental validation of micro-milling cutting forces of AISI H13 steel at hardness between 35 and 60 HRC. Int J Adv Manuf Technol 62:887–899. https://doi.org/10.1007/s00170-011-3864-7
81. Li H, Lai X, Li C et al (2008) Modelling and experimental analysis of the effects of tool wear, minimum chip thickness and micro tool geometry on the surface roughness in micro-end-milling. J Micromech Microeng 18:025006. https://doi.org/10.1088/0960-1317/18/2/025006
82. Singh KK, Singh R (2018) Chatter stability prediction in high-speed micromilling of Ti6Al4V via finite element based microend mill dynamics. Adv Manuf 6:95–106. https://doi.org/10.1007/s40436-018-0210-4
83. Balázs BZ, Takács M (2018) Finite element modelling of thin chip removal process. IOP Conf Ser: Mater Sci Eng 426:012002. https://doi.org/10.1088/1757-899X/426/1/012002
84. Bissacco G, Hansen HN, De Chiffre L (2006) Size effects on surface generation in micro milling of hardened tool steel. CIRP Ann Manuf Technol 55:593–596. https://doi.org/10.1016/S0007-8506(07)60490-9
85. Mian AJ, Driver N, Mativenga PT (2011) Identification of factors that dominate size effect in micro-machining. Int J Mach Tools Manuf 51:383–394. https://doi.org/10.1016/j.ijmachtools.2011.01.004
86. Pratap T, Patra K, Dyakonov AA (2015) Modeling cutting force in micro-milling of Ti-6Al-4V titanium alloy. Procedia Eng 129:134–139. https://doi.org/10.1016/j.proeng.2015.12.021
87. Uhlmann E, Oberschmidt D, Kuche Y, Löwenstein A (2014) Cutting edge preparation of micro milling tools. Procedia CIRP 14:349–354. https://doi.org/10.1016/j.procir.2014.03.083
88. Ramos AC, Autenrieth H, Strauß T et al (2012) Characterization of the transition from ploughing to cutting in micro machining and evaluation of the minimum thickness of cut. J Mater Process Technol 212:594–600. https://doi.org/10.1016/j.jmatprotec.2011.07.007
89. Kang I-S, Kim J-S, Seo Y-W (2010) Investigation of cutting force behaviour considering the effect of cutting edge radius in the micro-scale milling of AISI 1045 steel. Proc Inst Mech Eng B J Eng Manuf. https://doi.org/10.1243/09544054JEM1762
90. Vogler MP, DeVor RE, Kapoor SG (2005) On the modeling and analysis of machining performance in micro-endmilling, part i: surface generation. J Manuf Sci Eng 126:685–694. https://doi.org/10.1115/1.1813470
91. Lai X, Li H, Li C et al (2008) Modelling and analysis of micro scale milling considering size effect, micro cutter edge radius and minimum chip thickness. Int J Mach Tools Manuf 48:1–14. https://doi.org/10.1016/j.ijmachtools.2007.08.011
92. Malekian M, Mostofa MG, Park SS, Jun MBG (2012) Modeling of minimum uncut chip thickness in micro machining of aluminum. J Mater Process Technol 212:553–559. https://doi.org/10.1016/j.jmatprotec.2011.05.022
93. Son SM, Lim HS, Ahn JH (2005) Effects of the friction coefficient on the minimum cutting thickness in micro cutting. Int J Mach Tools Manuf 45:529–535. https://doi.org/10.1016/j.ijmachtools.2004.09.001
94. Aslantas K, Hopa HE, Percin M et al (2016) Cutting performance of nano-crystalline diamond (NCD) coating in micro-milling of Ti6Al4V alloy. Precis Eng 45:55–66. https://doi.org/10.1016/j.precisioneng.2016.01.009
95. Yang K, Liang Y, Zheng K et al (2011) Tool edge radius effect on cutting temperature in micro-end-milling process. Int J Adv Manuf Technol 52:905–912. https://doi.org/10.1007/s00170-010-2795-z
96. Woon KS, Rahman M, Fang FZ et al (2008) Investigations of tool edge radius effect in micromachining: a FEM simulation approach. J Mater Process Technol 195:204–211. https://doi.org/10.1016/j.jmatprotec.2007.04.137
97. Yuan ZJ, Zhou M, Dong S (1996) Effect of diamond tool sharpness on minimum cutting thickness and cutting surface integrity in

ultraprecision machining. J Mater Process Technol 62:327–330. https://doi.org/10.1016/S0924-0136(96)02429-6
98. Kiswanto G, Zariatin DL, Ko TJ (2014) The effect of spindle speed, feed-rate and machining time to the surface roughness and burr formation of aluminum alloy 1100 in micro-milling operation. J Manuf Process 16:435–450. https://doi.org/10.1016/j.jmapro.2014.05.003
99. Kumar P, Kumar M, Bajpai V, Singh NK (2017) Recent advances in characterization, modeling and control of burr formation in micro-milling. Manuf Lett 13:1–5. https://doi.org/10.1016/j.mfglet.2017.04.002
100. Geier N, Szalay T, Takács M (2019) Analysis of thrust force and characteristics of uncut fibres at non-conventional oriented drilling of unidirectional carbon fibre-reinforced plastic (UD-CFRP) composite laminates. Int J Adv Manuf Technol 100:3139–3154. https://doi.org/10.1007/s00170-018-2895-8
101. Ni C, Chen M, Wu C et al (2017) Research in minimum undeformed chip thickness and size effect in micro end-milling of potassium dihydrogen phosphate crystal. Int J Mech Sci. https://doi.org/10.1016/j.ijmecsci.2017.10.025
102. Wang JJ, Uhlmann E, Oberschmidt D et al (2016) Critical depth of cut and asymptotic spindle speed for chatter in micro milling with process damping. CIRP Ann Manuf Technol 65:113–116. https://doi.org/10.1016/j.cirp.2016.04.088
103. Geier N, Szalay T, Biró I (2018) Trochoid milling of carbon fibre-reinforced plastics (CFRP). Procedia CIRP 77:375–378. https://doi.org/10.1016/j.procir.2018.09.039
104. Gillespie LK, Blotter PT (1976) The formation and properties of machining burrs. J Eng Ind 98:66–74. https://doi.org/10.1115/1.3438875
105. Aurich JC, Dornfeld D, Arrazola PJ et al (2009) Burrs—analysis, control and removal. CIRP Ann Manuf Technol 58:519–542. https://doi.org/10.1016/j.cirp.2009.09.004
106. Lee K, Dornfeld DA (2005) Micro-burr formation and minimization through process control. Precis Eng 29:246–252. https://doi.org/10.1016/j.precisioneng.2004.09.002
107. Hashimura M, Hassamontr J, Dornfeld DA (1999) Effect of in-plane exit angle and rake angles on burr height and thickness in face milling operation. J Manuf Sci Eng 121:13–19. https://doi.org/10.1115/1.2830566
108. Oliaei SNB, Karpat Y (2017) Built-up edge effects on process outputs of titanium alloy micro milling. Precis Eng 49:305–315. https://doi.org/10.1016/j.precisioneng.2017.02.019
109. Saptaji K, Subbiah S (2017) Burr reduction of micro-milled microfluidic channels mould using a tapered tool. Procedia Eng 184:137–144. https://doi.org/10.1016/j.proeng.2017.04.078
110. Wu X, Li L, He N (2017) Investigation on the burr formation mechanism in micro cutting. Precis Eng 47:191–196. https://doi.org/10.1016/j.precisioneng.2016.08.004
111. Biermann D, Steiner M (2012) Analysis of micro burr formation in austenitic stainless steel X5CrNi18-10. Procedia CIRP 3:97–102. https://doi.org/10.1016/j.procir.2012.07.018
112. Piquard R, D'Acunto A, Laheurte P, Dudzinski D (2014) Micro-end milling of NiTi biomedical alloys, burr formation and phase transformation. Precis Eng 38:356–364. https://doi.org/10.1016/j.precisioneng.2013.11.006
113. Chen MJ, Ni HB, Wang ZJ, Jiang Y (2012) Research on the modeling of burr formation process in micro-ball end milling operation on Ti–6Al–4V. Int J Adv Manuf Technol 62:901–912. https://doi.org/10.1007/s00170-011-3865-6
114. Komatsu T, Yoshino T, Matsumura T, Torizuka S (2012) Effect of crystal grain size in stainless steel on cutting process in micromilling. Procedia CIRP 1:150–155. https://doi.org/10.1016/j.procir.2012.04.026
115. Kou Z, Wan Y, Cai Y et al (2015) Burr controlling in micro milling with supporting material method. Procedia Manuf 1:501–511. https://doi.org/10.1016/j.promfg.2015.09.015
116. Saptaji K, Subbiah S, Dhupia JS (2012) Effect of side edge angle and effective rake angle on top burrs in micro-milling. Precis Eng 36:444–450. https://doi.org/10.1016/j.precisioneng.2012.01.008
117. Yuan Y, Jing X, Ehmann KF et al (2018) Modeling of cutting forces in micro end-milling. J Manuf Process 31:844–858. https://doi.org/10.1016/j.jmapro.2018.01.012
118. Geier N, Szalay T (2017) Optimisation of process parameters for the orbital and conventional drilling of uni-directional carbon fibre-reinforced polymers (UD-CFRP). Measurement 110:319–334. https://doi.org/10.1016/j.measurement.2017.07.007
119. Afazov SM, Zdebski D, Ratchev SM et al (2013) Effects of micro-milling conditions on the cutting forces and process stability. J Mater Process Technol 213:671–684. https://doi.org/10.1016/j.jmatprotec.2012.12.001
120. Wu X, Li L, He N et al (2016) Influence of the cutting edge radius and the material grain size on the cutting force in micro cutting. Precis Eng 45:359–364. https://doi.org/10.1016/j.precisioneng.2016.03.012
121. Yun HT, Heo S, Lee MK et al (2011) Ploughing detection in micromilling processes using the cutting force signal. Int J Mach Tools Manuf 51:377–382. https://doi.org/10.1016/j.ijmachtools.2011.01.003
122. Simoneau A, Ng E, Elbestawi MA (2006) Chip formation during microscale cutting of a medium carbon steel. Int J Mach Tools Manuf 46:467–481. https://doi.org/10.1016/j.ijmachtools.2005.07.019
123. Zhou L, Peng F, Yan R et al (2015) Prediction and experimental validation of micro end-milling forces with finite element method. In: Intelligent Robotics and Applications. Springer, Cham, pp 664–675
124. Ahmadi M, Karpat Y, Acar O, Kalay YE (2018) Microstructure effects on process outputs in micro scale milling of heat treated Ti6Al4V titanium alloys. J Mater Process Technol 252:333–347. https://doi.org/10.1016/j.jmatprotec.2017.09.042
125. Wissmiller DL, Pfefferkorn FE (2009) Micro end mill tool temperature measurement and prediction. J Manuf Process 11:45–53. https://doi.org/10.1016/j.jmapro.2009.06.001
126. Mamedov A, Lazoglu I (2016) Thermal analysis of micro milling titanium alloy Ti–6Al–4V. J Mater Process Technol 229:659–667. https://doi.org/10.1016/j.jmatprotec.2015.10.019
127. Bali J (1985) Forgácsolás. Tankönyvkiadó, Budapest
128. Uhlmann E, Piltz S, Schauer K (2005) Micro milling of sintered tungsten–copper composite materials. J Mater Process Technol 167:402–407. https://doi.org/10.1016/j.jmatprotec.2005.05.022
129. Thepsonthi T, Özel T (2013) Experimental and finite element simulation based investigations on micro-milling Ti-6Al-4V titanium alloy: Effects of cBN coating on tool wear. J Mater Process Technol 213:532–542. https://doi.org/10.1016/j.jmatprotec.2012.11.003
130. Munoa J, Beudaert X, Dombovari Z et al (2016) Chatter suppression techniques in metal cutting. CIRP Ann 65:785–808. https://doi.org/10.1016/j.cirp.2016.06.004
131. Hajdu D, Insperger T, Stepan G (2017) Robust stability analysis of machining operations. Int J Adv Manuf Technol 88:45–54. https://doi.org/10.1007/s00170-016-8715-0
132. Kiss AK, Hajdu D, Bachrathy D, Stepan G (2018) Operational stability prediction in milling based on impact tests. Mech Syst Signal Process 103:327–339. https://doi.org/10.1016/j.ymssp.2017.10.019
133. Ma L, Howard I, Pang M et al (2020) Experimental investigation of cutting vibration during micro-end-milling of the straight groove. Micromachines 11:494. https://doi.org/10.3390/mi11050494

134. Singh KK, Kartik V, Singh R (2015) Modeling dynamic stability in high-speed micromilling of Ti–6Al–4V via velocity and chip load dependent cutting coefficients. Int J Mach Tools Manuf 96: 56–66. https://doi.org/10.1016/j.ijmachtools.2015.06.002
135. Biró I, Szalay T, Geier N (2018) Effect of cutting parameters on section borders of the empirical specific cutting force model for cutting with micro-sized uncut chip thickness. Procedia CIRP 77: 279–282. https://doi.org/10.1016/j.procir.2018.09.015
136. Tlusty J, Ismail F (1983) Special aspects of chatter in milling. J Vib Acoust Stress Reliab Des 105:24–32. https://doi.org/10.1115/1.3269061
137. Susanto A, Liu C-H, Yamada K et al (2018) Application of Hilbert–Huang transform for vibration signal analysis in end-milling. Precis Eng 53:263–277. https://doi.org/10.1016/j.precisioneng.2018.04.008
138. Yang Y, Zhang W-H, Ma Y-C, Wan M (2016) Chatter prediction for the peripheral milling of thin-walled workpieces with curved surfaces. Int J Mach Tools Manuf 109:36–48. https://doi.org/10.1016/j.ijmachtools.2016.07.002
139. Afazov SM, Ratchev SM, Segal J, Popov AA (2012) Chatter modelling in micro-milling by considering process nonlinearities. Int J Mach Tools Manuf 56:28–38. https://doi.org/10.1016/j.ijmachtools.2011.12.010
140. Biermann D, Baschin A (2009) Influence of cutting edge geometry and cutting edge radius on the stability of micromilling processes. Prod Eng Res Devel 3:375. https://doi.org/10.1007/s11740-009-0188-7
141. Quintana G, Ciurana J (2011) Chatter in machining processes: a review. Int J Mach Tools Manuf 51:363–376. https://doi.org/10.1016/j.ijmachtools.2011.01.001
142. Mamedov A, Layegh KSE, Lazoglu I (2013) Machining forces and tool deflections in micro milling. Procedia CIRP 8:147–151. https://doi.org/10.1016/j.procir.2013.06.080
143. Jun MB, Liu X, DeVor RE, Kapoor SG (2006) Investigation of the dynamics of microend milling—part i: model development. J Manuf Sci Eng 128:893–900. https://doi.org/10.1115/1.2193546
144. Mokhtari A, Jalili MM, Mazidi A, Abootorabi MM (2019) Size dependent vibration analysis of micro-milling operations with process damping and structural nonlinearities. Eur J Mech - A/Solids 76:57–69. https://doi.org/10.1016/j.euromechsol.2019.03.009
145. Sahoo P, Patra K, Singh VK et al (2019) Influences of TiAlN coating and limiting angles of flutes on prediction of cutting forces and dynamic stability in micro milling of die steel (P-20). J Mater Process Technol 116500. https://doi.org/10.1016/j.jmatprotec.2019.116500
146. Uhlmann E, Oberschmidt D, Löwenstein A, Kuche Y (2016) Influence of cutting edge preparation on the performance of micro milling tools. Procedia CIRP 46:214–217. https://doi.org/10.1016/j.procir.2016.03.204
147. Li K-M, Chou S-Y (2010) Experimental evaluation of minimum quantity lubrication in near micro-milling. J Mater Process Technol 210:2163–2170. https://doi.org/10.1016/j.jmatprotec.2010.07.031
148. Zhang X, Yu T, Wang W (2018) Prediction of cutting forces and instantaneous tool deflection in micro end milling by considering tool run-out. Int J Mech Sci 136:124–133. https://doi.org/10.1016/j.ijmecsci.2017.12.019
149. Oliaei SNB, Karpat Y (2014) Experimental investigations on micro milling of Stavax stainless steel. Procedia CIRP 14:377–382. https://doi.org/10.1016/j.procir.2014.03.006
150. Wang Y, Zou B, Wang J et al (2020) Effect of the progressive tool wear on surface topography and chip formation in micro-milling of Ti–6Al–4V using Ti(C7N3)-based cermet micro-mill. Tribol Int 141:105900. https://doi.org/10.1016/j.triboint.2019.105900
151. Vipindas K, Mathew J (2019) Wear behavior of TiAlN coated WC tool during micro end milling of Ti-6Al-4V and analysis of surface roughness. Wear 424–425:165–182. https://doi.org/10.1016/j.wear.2019.02.018
152. Kim JS, Kim JW, Lee SW (2017) Experimental characterization on micro-end milling of titanium alloy using nanofluid minimum quantity lubrication with chilly gas. Int J Adv Manuf Technol 91: 2741–2749. https://doi.org/10.1007/s00170-016-9965-6
153. Klocke F, Eisenblätter G (1997) Dry cutting. CIRP Ann 46:519–526. https://doi.org/10.1016/S0007-8506(07)60877-4
154. Ginting A, Nouari M (2009) Surface integrity of dry machined titanium alloys. Int J Mach Tools Manuf 49:325–332. https://doi.org/10.1016/j.ijmachtools.2008.10.011
155. Ziberov M, da Silva MB, Jackson M, Hung WNP (2016) Effect of cutting fluid on micromilling of Ti-6Al-4V titanium alloy. Procedia Manuf 5:332–347. https://doi.org/10.1016/j.promfg.2016.08.029
156. Aslantas K, Çicek A, Ucun İ et al (2016) Performance evaluation of a hybrid cooling–lubrication system in micro-milling of Ti6Al4V alloy. Procedia CIRP 46:492–495. https://doi.org/10.1016/j.procir.2016.04.037
157. Li P (2009) Micromilling of hardened tool steels - Proefschrift
158. Lu X, Hu X, Jia Z et al (2018) Model for the prediction of 3D surface topography and surface roughness in micro-milling Inconel 718. Int J Adv Manuf Technol 94:2043–2056. https://doi.org/10.1007/s00170-017-1001-y
159. Lu X, Jia Z, Lu Y et al (2017) Predicting the surface hardness of micro-milled nickel-base superalloy Inconel 718. Int J Adv Manuf Technol 93:1283–1292. https://doi.org/10.1007/s00170-017-0512-x
160. Zhang S, Li JF, Wang YW (2012) Tool life and cutting forces in end milling Inconel 718 under dry and minimum quantity cooling lubrication cutting conditions. J Clean Prod 32:81–87. https://doi.org/10.1016/j.jclepro.2012.03.014
161. Zheng WH (2008) The machining technology of hard cutting material. National defence of Industry Press, Bejing
162. Göransson A, Jansson E, Tengvall P, Wennerberg A (2003) Bone formation after 4 weeks around blood-plasma-modified titanium implants with varying surface topographies: an in vivo study. Biomaterials 24:197–205. https://doi.org/10.1016/S0142-9612(02)00277-6
163. Lee TM, Chang E, Yang CY (2004) Attachment and proliferation of neonatal rat calvarial osteoblasts on Ti6Al4V: effect of surface chemistries of the alloy. Biomaterials 25:23–32. https://doi.org/10.1016/S0142-9612(03)00465-4
164. Sartkulvanich P, Koppka F, Altan T (2004) Determination of flow stress for metal cutting simulation—a progress report. J Mater Process Technol 146:61–71. https://doi.org/10.1016/S0924-0136(03)00845-8
165. Davies MA, Cao Q, Cooks AL, Ivester R (2003) On the measurement and prediction of temperature fields in machining AISI 1045 steel. CIRP Ann 52:77–80. https://doi.org/10.1016/S0007-8506(07)60535-6
166. Simoneau A, Ng E, Elbestawi MA (2006) Surface defects during microcutting. Int J Mach Tools Manuf 46:1378–1387. https://doi.org/10.1016/j.ijmachtools.2005.10.001
167. Takács M, Verö B, Mészáros I (2003) Micromilling of metallic materials. J Mater Process Technol 138:152–155. https://doi.org/10.1016/S0924-0136(03)00064-5
168. Chen W, Huo D, Teng X, Sun Y (2017) Surface generation modelling for micro end milling considering the minimum chip thickness and tool runout. Procedia CIRP 58:364–369. https://doi.org/10.1016/j.procir.2017.03.237
169. Rodríguez P, Labarga JE (2013) A new model for the prediction of cutting forces in micro-end-milling operations. J Mater Process Technol 213:261–268. https://doi.org/10.1016/j.jmatprotec.2012.09.009

170. Afazov SM, Ratchev SM, Segal J (2010) Modelling and simulation of micro-milling cutting forces. J Mater Process Technol 210: 2154–2162. https://doi.org/10.1016/j.jmatprotec.2010.07.033
171. Biró I, Szalay T (2017) Extension of empirical specific cutting force model for the process of fine chip-removing milling. Int J Adv Manuf Technol 88:2735–2743. https://doi.org/10.1007/s00170-016-8957-x
172. Peng FY, Dong Q, Yan R et al (2016) Analytical modeling and experimental validation of residual stress in micro-end-milling. Int J Adv Manuf Technol 87:3411–3424. https://doi.org/10.1007/s00170-016-8697-y
173. Zhou L, Peng FY, Yan R et al (2015) Analytical modeling and experimental validation of micro end-milling cutting forces considering edge radius and material strengthening effects. Int J Mach Tools Manuf 97:29–41. https://doi.org/10.1016/j.ijmachtools.2015.07.001
174. Zhou L, Deng B, Peng F et al (2020) Semi-analytic modelling of cutting forces in micro ball-end milling of NAK80 steel with wear-varying cutting edge and associated nonlinear process characteristics. Int J Mech Sci 169:105343. https://doi.org/10.1016/j.ijmecsci.2019.105343
175. Kumar M, Dotson K, Melkote SN (2010) An experimental technique to detect tool–workpiece contact in micromilling. J Manuf Process 12:99–105. https://doi.org/10.1016/j.jmapro.2010.08.001
176. Hsieh W-H, Lu M-C, Chiou S-J (2012) Application of backpropagation neural network for spindle vibration-based tool wear monitoring in micro-milling. Int J Adv Manuf Technol 61: 53–61. https://doi.org/10.1007/s00170-011-3703-x
177. Balázs BZ, Jacsó Á, Takács M (2020) Micromachining of hardened hot-work tool steel: effects of milling strategies. Int J Adv Manuf Technol. https://doi.org/10.1007/s00170-020-05561-x
178. Lauro CH, Ribeiro Filho SLM, Baldo D et al (2016) Optimization of micro milling of hardened steel with different grain sizes using multi-objective evolutionary algorithm. Measurement 85:88–99. https://doi.org/10.1016/j.measurement.2016.02.011
179. Saklakoglu IE, Kasman S (2011) Investigation of micro-milling process parameters for surface roughness and milling depth. Int J Adv Manuf Technol 54:567–578. https://doi.org/10.1007/s00170-010-2953-3
180. Manso CS, Thom S, Uhlmann E et al (2019) Tool wear modelling using micro tool diameter reduction for micro-end-milling of tool steel H13. Int J Adv Manuf Technol 105:2531–2542. https://doi.org/10.1007/s00170-019-04575-4
181. Saedon JB, Soo SL, Aspinwall DK et al (2012) Prediction and optimization of tool life in micromilling AISI D2 (~62 HRC) hardened steel. Procedia Eng 41:1674–1683. https://doi.org/10.1016/j.proeng.2012.07.367
182. Sredanovic B, Globocki Lakic G, Kramar D, Kopac J (2016) Analysis of micro-milling of hardened tool steel. Key Engineering Materials, In https://www.scientific.net/KEM.686.57.
183. Micromilling of hardened (62HRC) AISI D2 cold work tool steel - Saedon12PhD.pdf. http://etheses.bham.ac.uk/3390/1/Saedon12PhD.pdf. Accessed 26 Mar 2017
184. Venkata Rao K (2019) Power consumption optimization strategy in micro ball-end milling of D2 steel via TLBO coupled with 3D FEM simulation. Measurement 132:68–78. https://doi.org/10.1016/j.measurement.2018.09.044
185. Chi-Hsiang C, Yung-Cheng W, Bean-Yin L (2013) The optimal design of micro end mill for milling SKD61 tool steel. Int J Adv Manuf Technol 68:165–173. https://doi.org/10.1007/s00170-012-4716-9
186. Wojciechowski S, Maruda RW, Nieslony P, Krolczyk GM (2016) Investigation on the edge forces in ball end milling of inclined surfaces. Int J Mech Sci 119:360–369. https://doi.org/10.1016/j.ijmecsci.2016.10.034
187. Jemielniak K, Arrazola PJ (2008) Application of AE and cutting force signals in tool condition monitoring in micro-milling. CIRP J Manuf Sci Technol 1:97–102. https://doi.org/10.1016/j.cirpj.2008.09.007
188. Jemielniak K, Bombiński S, Aristimuno PX (2008) Tool condition monitoring in micromilling based on hierarchical integration of signal measures. CIRP Ann 57:121–124. https://doi.org/10.1016/j.cirp.2008.03.053
189. Ren Q, Balazinski M, Baron L et al (2014) Type-2 fuzzy tool condition monitoring system based on acoustic emission in micromilling. Inf Sci 255:121–134. https://doi.org/10.1016/j.ins.2013.06.010
190. Xu X, Huang S, Wang M, Yao W (2017) A study on process parameters in end milling of AISI-304 stainless steel under electrostatic minimum quantity lubrication conditions. Int J Adv Manuf Technol 90:979–989. https://doi.org/10.1007/s00170-016-9417-3
191. Peng Z, Li J, Yan P et al (2017) Experimental and simulation research on micro-milling temperature and cutting deformation of heat-resistance stainless steel. Int J Adv Manuf Technol:1–14. https://doi.org/10.1007/s00170-017-1091-6
192. De Cristofaro S, Funaro N, Feriti GC et al (2012) High-speed micro-milling: novel coatings for tool wear reduction. Int J Mach Tools Manuf 63:16–20. https://doi.org/10.1016/j.ijmachtools.2012.07.005
193. Alhadeff LL, Marshall MB, Curtis DT, Slatter T (2019) Protocol for tool wear measurement in micro-milling. Wear 420–421:54–67. https://doi.org/10.1016/j.wear.2018.11.018
194. Wan Z, Li Y, Tang H et al (2014) Characteristics and mechanism of top burr formation in slotting microchannels using arrayed thin slotting cutters. Precis Eng 38:28–35. https://doi.org/10.1016/j.precisioneng.2013.06.008
195. Romoli L (2017) Flattening of surface roughness in ultrashort pulsed laser micro-milling. Precis Eng. https://doi.org/10.1016/j.precisioneng.2017.09.003
196. Ding H, Shen N, Shin YC (2012) Thermal and mechanical modeling analysis of laser-assisted micro-milling of difficult-to-machine alloys. J Mater Process Technol 212:601–613. https://doi.org/10.1016/j.jmatprotec.2011.07.016
197. Schaller T, Bohn L, Mayer J, Schubert K (1999) Microstructure grooves with a width of less than 50 μm cut with ground hard metal micro end mills. Precis Eng 23:229–235. https://doi.org/10.1016/S0141-6359(99)00011-2
198. Selaimia A-A, Yallese MA, Bensouilah H et al (2017) Modeling and optimization in dry face milling of X2CrNi18-9 austenitic stainless steel using RMS and desirability approach. Measurement 107:53–67. https://doi.org/10.1016/j.measurement.2017.05.012
199. Zaman MT, Kumar AS, Rahman M, Sreeram S (2006) A three-dimensional analytical cutting force model for micro end milling operation. Int J Mach Tools Manuf 46:353–366. https://doi.org/10.1016/j.ijmachtools.2005.05.021
200. Lu X, Jia Z, Wang H et al (2019) The effect of cutting parameters on micro-hardness and the prediction of Vickers hardness based on a response surface methodology for micro-milling Inconel 718. Measurement 140:56–62. https://doi.org/10.1016/j.measurement.2019.03.037
201. Lu X, Wang F, Wang X, et al (2017) A surface roughness prediction model using response surface methodology in micro-milling Inconel 718. IJMMM 19:230. https://doi.org/10.1504/IJMMM.2017.084006
202. Lu X, Jia Z, Wang X et al (2015) Three-dimensional dynamic cutting forces prediction model during micro-milling nickel-based superalloy. Int J Adv Manuf Technol 81:2067–2086. https://doi.org/10.1007/s00170-015-7310-0

203. Wang C, Li K, Chen M, Liu Z (2015) Evaluation of minimum quantity lubrication effects by cutting force signals in face milling of Inconel 182 overlays. Journal of Cleaner Production 108, Part A:145–157. https://doi.org/10.1016/j.jclepro.2015.06.095
204. Chen N, Yuan Y, Guo C et al (2020) Design, optimization and manufacturing of polycrystalline diamond micro-end-mill for micro-milling of GH4169. Diam Relat Mater 108:107915. https://doi.org/10.1016/j.diamond.2020.107915
205. Gao Q, Gong Y, Zhou Y, Wen X (2017) Experimental study of micro-milling mechanism and surface quality of a nickel-based single crystal superalloy. J Mech Sci Technol 31:171–180. https://doi.org/10.1007/s12206-016-1218-y
206. Zain AM, Haron H, Sharif S (2010) Prediction of surface roughness in the end milling machining using Artificial Neural Network. Expert Syst Appl 37:1755–1768. https://doi.org/10.1016/j.eswa.2009.07.033
207. Mamedov A, K SEL, Lazoglu I (2015) Instantaneous tool deflection model for micro milling. Int J Adv Manuf Technol 79:769–777. https://doi.org/10.1007/s00170-015-6877-9
208. Mittal RK, Kulkarni SS, Singh R (2018) Characterization of lubrication sensitivity on dynamic stability in high-speed micromilling of Ti–6Al–4V via a novel numerical scheme. Int J Mech Sci 142–143:51–65. https://doi.org/10.1016/j.ijmecsci.2018.04.038
209. Sahoo P, Pratap T, Patra K (2019) A hybrid modelling approach towards prediction of cutting forces in micro end milling of Ti-6Al-4V titanium alloy. Int J Mech Sci 150:495–509. https://doi.org/10.1016/j.ijmecsci.2018.10.032
210. Wang Y, Zou B, Huang C et al (2019) Feasibility study of the Ti(C7N3)-based cermet micro-mill based on dynamic fatigue behavior and modeling of the contact stress distribution on the round cutting edge. Int J Mech Sci 155:143–158. https://doi.org/10.1016/j.ijmecsci.2019.02.038
211. Vazquez E, Gomar J, Ciurana J, Rodríguez CA (2015) Analyzing effects of cooling and lubrication conditions in micromilling of Ti6Al4V. J Clean Prod 87:906–913. https://doi.org/10.1016/j.jclepro.2014.10.016
212. Chen W, Teng X, Zheng L et al (2018) Burr reduction mechanism in vibration-assisted micro milling. Manuf Lett 16:6–9. https://doi.org/10.1016/j.mfglet.2018.02.015
213. Dadgari A, Huo D, Swailes D (2018) Investigation on tool wear and tool life prediction in micro-milling of Ti-6Al-4V. Nanotechnol Precis Eng 1:218–225. https://doi.org/10.1016/j.npe.2018.12.005
214. Colpani A, Fiorentino A, Ceretti E, Attanasio A (2019) Tool wear analysis in micromilling of titanium alloy. Precis Eng. https://doi.org/10.1016/j.precisioneng.2019.03.011
215. Yadav AK, Kumar M, Bajpai V et al (2017) FE modeling of burr size in high- speed micro-milling of Ti6Al4V. Precis Eng 49:287–292. https://doi.org/10.1016/j.precisioneng.2017.02.017
216. Jing X, Lv R, Chen Y et al (2020) Modelling and experimental analysis of the effects of run out, minimum chip thickness and elastic recovery on the cutting force in micro-end-milling. Int J Mech Sci 176:105540. https://doi.org/10.1016/j.ijmecsci.2020.105540
217. Oliaei SNB, Karpat Y (2019) Modelling and analysis of tool deflections in tailored micro end mills. IJMMS 12:20. https://doi.org/10.1504/IJMMS.2019.097843
218. Miranda M, Serje D, Pacheco J, Bris J (2018) Tool edge radius wear and material removal rate performance charts for titanium micro-milling. Int J Precis Eng Manuf 19:79–84. https://doi.org/10.1007/s12541-018-0009-z
219. Medeossi F, Sorgato M, Bruschi S, Savio E (2018) Novel method for burrs quantitative evaluation in micro-milling. Precis Eng 54:379–387. https://doi.org/10.1016/j.precisioneng.2018.07.007
220. Uhlmann E, Oberschmidt D, Kuche Y et al (2016) Effects of different cutting edge preparation methods on micro milling performance. Procedia CIRP 46:352–355. https://doi.org/10.1016/j.procir.2016.04.004
221. Kieren-Ehses S, Bohley M, Arrabiyeh P et al (2018) Influence of different metal working fluids when micro machining cp-titanium with 50 μm diameter micro end mills. Procedia CIRP 71:198–202. https://doi.org/10.1016/j.procir.2018.05.097
222. Liu H, Sun Y, Geng Y, Shan D (2015) Experimental research of milling force and surface quality for TC4 titanium alloy of micro-milling. Int J Adv Manuf Technol 79:705–716. https://doi.org/10.1007/s00170-015-6844-5
223. Bandapalli C, Sutaria BM, Prasad Bhatt DV, Singh KK (2018) Tool wear analysis of micro end mills-uncoated and PVD coated TiAlN & AlTiN in high speed micro milling of titanium alloy-Ti-0.3Mo-0.8Ni. Procedia CIRP 77:626–629. https://doi.org/10.1016/j.procir.2018.08.191
224. Filiz S, Conley CM, Wasserman MB, Ozdoganlar OB (2007) An experimental investigation of micro-machinability of copper 101 using tungsten carbide micro-endmills. Int J Mach Tools Manuf 47:1088–1100. https://doi.org/10.1016/j.ijmachtools.2006.09.024
225. Li K, Zhu K, Mei T (2016) A generic instantaneous undeformed chip thickness model for the cutting force modeling in micromilling. Int J Mach Tools Manuf 105:23–31. https://doi.org/10.1016/j.ijmachtools.2016.03.002
226. Rahman M, Senthil Kumar A, Prakash JRS (2001) Micro milling of pure copper. J Mater Process Technol 116:39–43. https://doi.org/10.1016/S0924-0136(01)00848-2
227. Zhu K, Wong YS, Hong GS (2009) Multi-category micro-milling tool wear monitoring with continuous hidden Markov models. Mech Syst Signal Process 23:547–560. https://doi.org/10.1016/j.ymssp.2008.04.010
228. Min S, Dornfeld D, Inasaki I et al (2006) Variation in machinability of single crystal materials in micromachining. CIRP Ann Manuf Technol 55:103–106. https://doi.org/10.1016/S0007-8506(07)60376-X
229. Kim C-J, Mayor JR, Ni J (2005) A static model of chip formation in microscale milling. J Manuf Sci Eng 126:710–718. https://doi.org/10.1115/1.1813475
230. Shi Y, Mahr F, von Wagner U, Uhlmann E (2012) Chatter frequencies of micromilling processes: influencing factors and online detection via piezoactuators. Int J Mach Tools Manuf 56:10–16. https://doi.org/10.1016/j.ijmachtools.2011.12.001
231. Vázquez E, Rodríguez CA, Elías-Zúñiga A, Ciurana J (2010) An experimental analysis of process parameters to manufacture metallic micro-channels by micro-milling. Int J Adv Manuf Technol 51:945–955. https://doi.org/10.1007/s00170-010-2685-4
232. Chen W, Teng X, Huo D, Wang Q (2017) An improved cutting force model for micro milling considering machining dynamics. Int J Adv Manuf Technol 93:3005–3016. https://doi.org/10.1007/s00170-017-0706-2
233. Malekian M, Park SS, Jun MBG (2009) Modeling of dynamic micro-milling cutting forces. Int J Mach Tools Manuf 49:586–598. https://doi.org/10.1016/j.ijmachtools.2009.02.006
234. Zhang X, Ehmann KF, Yu T, Wang W (2016) Cutting forces in micro-end-milling processes. Int J Mach Tools Manuf 107:21–40. https://doi.org/10.1016/j.ijmachtools.2016.04.012
235. Sun Z, To S, Zhang S, Zhang G (2018) Theoretical and experimental investigation into non-uniformity of surface generation in micro-milling. Int J Mech Sci 140:313–324. https://doi.org/10.1016/j.ijmecsci.2018.03.019
236. Chen W, Zheng L, Xie W et al (2019) Modelling and experimental investigation on textured surface generation in vibration-assisted micro-milling. J Mater Process Technol 266:339–350. https://doi.org/10.1016/j.jmatprotec.2018.11.011

237. Friedrich CR, Kulkarni VP (2004) Effect of workpiece springback on micromilling forces. Microsyst Technol 10:472–477. https://doi.org/10.1007/s00542-004-0375-6
238. Chern G-L, Wu Y-JE, Cheng J-C, Yao J-C (2007) Study on burr formation in micro-machining using micro-tools fabricated by micro-EDM. Precis Eng 31:122–129. https://doi.org/10.1016/j.precisioneng.2006.04.001
239. Zhang X, Yu T, Zhao J (2020) Surface generation modeling of micro milling process with stochastic tool wear. Precis Eng 61:170–181. https://doi.org/10.1016/j.precisioneng.2019.10.015
240. Park SS, Malekian M (2009) Mechanistic modeling and accurate measurement of micro end milling forces. CIRP Ann Manuf Technol 58:49–52. https://doi.org/10.1016/j.cirp.2009.03.060
241. Zheng L, Chiou YS, Liang SY (1996) Three dimensional cutting force analysis in end milling. Int J Mech Sci 38:259–269. https://doi.org/10.1016/0020-7403(95)00057-7
242. Kang IS, Kim JS, Kim JH et al (2007) A mechanistic model of cutting force in the micro end milling process. J Mater Process Technol 187–188:250–255. https://doi.org/10.1016/j.jmatprotec.2006.11.155
243. Newby G, Venkatachalam S, Liang SY (2007) Empirical analysis of cutting force constants in micro-end-milling operations. J Mater Process Technol 192–193:41–47. https://doi.org/10.1016/j.jmatprotec.2007.04.026
244. Rahnama R, Sajjadi M, Park SS (2009) Chatter suppression in micro end milling with process damping. J Mater Process Technol 209:5766–5776. https://doi.org/10.1016/j.jmatprotec.2009.06.009
245. Song Q, Liu Z, Shi Z (2014) Chatter stability for micromilling processes with flat end mill. Int J Adv Manuf Technol 71:1159–1174. https://doi.org/10.1007/s00170-013-5554-0
246. Xu K, Zou B, Wang Y et al (2016) An experimental investigation of micro-machinability of aluminum alloy 2024 using Ti(C7N3)-based cermet micro end-mill tools. J Mater Process Technol 235:13–27. https://doi.org/10.1016/j.jmatprotec.2016.04.011
247. Bissacco G, Hansen HN, Slunsky J (2008) Modelling the cutting edge radius size effect for force prediction in micro milling. CIRP Ann Manuf Technol 57:113–116. https://doi.org/10.1016/j.cirp.2008.03.085
248. Niu Z, Jiao F, Cheng K (2018) An innovative investigation on chip formation mechanisms in micro-milling using natural diamond and tungsten carbide tools. J Manuf Process 31:382–394. https://doi.org/10.1016/j.jmapro.2017.11.023
249. Davoudinejad A, Li D, Zhang Y, Tosello G (2019) Optimization of corner micro end milling by finite element modelling for machining thin features. Procedia CIRP 82:362–367. https://doi.org/10.1016/j.procir.2019.04.158
250. Mamedov A, Lazoglu I (2016) An evaluation of micro milling chip thickness models for the process mechanics. Int J Adv Manuf Technol 87:1843–1849. https://doi.org/10.1007/s00170-016-8584-6
251. Huo D, Lin C, Choong ZJ et al (2015) Surface and subsurface characterisation in micro-milling of monocrystalline silicon. Int J Adv Manuf Technol 81:1319–1331. https://doi.org/10.1007/s00170-015-7308-7
252. Rusnaldy KTJ, Kim HS (2007) Micro-end-milling of single-crystal silicon. Int J Mach Tools Manuf 47:2111–2119. https://doi.org/10.1016/j.ijmachtools.2007.05.003
253. Arif M, Rahman M, San WY (2012) An experimental investigation into micro ball end-milling of silicon. J Manuf Process 14:52–61. https://doi.org/10.1016/j.jmapro.2011.09.004
254. Choong ZJ, Huo D, Degenaar P, O'Neill A (2019) Micro-machinability and edge chipping mechanism studies on diamond micro-milling of monocrystalline silicon. J Manuf Process 38:93–103. https://doi.org/10.1016/j.jmapro.2019.01.004
255. Yang M, Peng F, Yan R et al (2019) Study on the surface damage mechanism of monocrystalline silicon in micro ball-end milling. Precis Eng 56:223–234. https://doi.org/10.1016/j.precisioneng.2018.12.003
256. Bhavsar SN, Aravindan S, Rao PV (2015) Investigating material removal rate and surface roughness using multi-objective optimization for focused ion beam (FIB) micro-milling of cemented carbide. Precis Eng 40:131–138. https://doi.org/10.1016/j.precisioneng.2014.10.014
257. Yuan H, Zhao W, Liang Z et al (2020) Structural design and fabrication of polycrystalline diamond micro ball-end mill. Int J Adv Manuf Technol 108:1899–1911. https://doi.org/10.1007/s00170-020-05436-1
258. Wu X, Li L, He N et al (2018) Study on the tool wear and its effect of PCD tool in micro milling of tungsten carbide. Int J Refract Met Hard Mater 77:61–67. https://doi.org/10.1016/j.ijrmhm.2018.07.010
259. Wu X, Li L, He N et al (2019) Investigation on the surface formation mechanism in micro milling of cemented carbide. Int J Refract Met Hard Mater 78:61–67. https://doi.org/10.1016/j.ijrmhm.2018.09.001
260. Huo D, Lin C, Dalgarno K (2014) An experimental investigation on micro machining of fine-grained graphite. Int J Adv Manuf Technol 72:943–953. https://doi.org/10.1007/s00170-014-5730-x
261. Huo D, Choong ZJ, Shi Y et al (2016) Diamond micro-milling of lithium niobate for sensing applications. J Micromech Microeng 26:095005. https://doi.org/10.1088/0960-1317/26/9/095005
262. Reichenbach IG, Bohley M, Sousa FJP, Aurich JC (2019) Tool-life criteria and wear behavior of single-edge ultra-small micro end mills. Precis Eng 55:48–58. https://doi.org/10.1016/j.precisioneng.2018.08.006
263. Jiao F, Cheng K (2014) An experimental investigation on micro-milling of polymethyl methacrylate components with nanometric surface roughness. Proc Inst Mech Eng B J Eng Manuf 228:790–796. https://doi.org/10.1177/0954405413507251
264. Oliaei SNB, Karpat Y (2018) Polycrystalline diamond end mill cutting edge design to improve ductile-mode machining of silicon. Precis Eng 51:403–414. https://doi.org/10.1016/j.precisioneng.2017.09.012
265. Lan T-H, Wang C-H, Chen K-K et al (2017) Milling properties of low temperature sintered zirconia blocks for dental use. Mater Sci Eng C 73:692–699. https://doi.org/10.1016/j.msec.2016.12.089
266. Romanus H, Ferraris E, Bouquet J et al (2014) Micromilling of sintered ZrO2 ceramic via cBN and diamond coated tools. Procedia CIRP 14:371–376. https://doi.org/10.1016/j.procir.2014.03.063
267. Arif M, Rahman M, San WY (2011) Ultraprecision ductile mode machining of glass by micromilling process. J Manuf Process 13:50–59. https://doi.org/10.1016/j.jmapro.2010.10.004
268. Mohanraj T, Shankar S, Rajasekar R et al (2020) Tool condition monitoring techniques in milling process—a review. J Mater Res Technol 9:1032–1042. https://doi.org/10.1016/j.jmrt.2019.10.031
269. Dimla DE (2000) Sensor signals for tool-wear monitoring in metal cutting operations—a review of methods. Int J Mach Tools Manuf 40:1073–1098. https://doi.org/10.1016/S0890-6955(99)00122-4
270. Móricz L, Viharos ZJ, Németh A et al (2020) Off-line geometrical and microscopic & on-line vibration based cutting tool wear analysis for micro-milling of ceramics. Measurement 163:108025. https://doi.org/10.1016/j.measurement.2020.108025
271. Saglam H, Unuvar A (2003) Tool condition monitoring in milling based on cutting forces by a neural network. Int J Prod Res 41:1519–1532. https://doi.org/10.1080/0020754031000073017
272. Hong GS, Rahman M, Zhou Q (1996) Using neural network for tool condition monitoring based on wavelet decomposition. Int J Mach Tools Manuf 36:551–566. https://doi.org/10.1016/0890-6955(95)00067-4

273. Malekian M, Park SS, Jun MBG (2009) Tool wear monitoring of micro-milling operations. J Mater Process Technol 209:4903–4914. https://doi.org/10.1016/j.jmatprotec.2009.01.013
274. Li W, Liu T (2019) Time varying and condition adaptive hidden Markov model for tool wear state estimation and remaining useful life prediction in micro-milling. Mech Syst Signal Process 131:689–702. https://doi.org/10.1016/j.ymssp.2019.06.021
275. Lu X, Wang F, Yang K, et al (2019) An indirect method for the measurement of micro-milling forces. American Society of Mechanical Engineers Digital Collection
276. Pratap T, Patra K (2018) Micro ball-end milling—an emerging manufacturing technology for micro-feature patterns. Int J Adv Manuf Technol 94:2821–2845. https://doi.org/10.1007/s00170-017-1064-9
277. Hao X, Chen M, Liu L et al (2020) Fabrication of large aspect ratio PCD micro-milling tool with pulsed lasers and grinding. J Manuf Process 58:489–499. https://doi.org/10.1016/j.jmapro.2020.08.032
278. Abolfazl Zahedi S, Demiral M, Roy A, Silberschmidt VV (2013) FE/SPH modelling of orthogonal micro-machining of f.c.c. single crystal. Comput Mater Sci 78:104–109. https://doi.org/10.1016/j.commatsci.2013.05.022
279. Lautenschlaeger MP, Stephan S, Urbassek HM, et al (2017) Effects of lubrication on the friction in nanometric machining processes: a molecular dynamics approach. In: Applied Mechanics and Materials. /AMM.869.85. Accessed 16 Jun 2020
280. Abaie MM, Zolfaghari M, Tahmasbi V, Karimi P (2020) Optimization of effective parameters on the nano-scale cutting process of monocrystalline copper using molecular dynamic. J Stress Anal 4:127–136. https://doi.org/10.22084/jrstan.2020.20790.1124
281. Karkalos NE, Markopoulos AP, Kundrák J (2018) 3D molecular dynamics model for nano-machining of fcc and bcc materials. Procedia CIRP 77:203–206. https://doi.org/10.1016/j.procir.2018.08.286
282. Xu Y, Wang M, Zhu F et al (2019) A molecular dynamic study of nano-grinding of a monocrystalline copper-silicon substrate. Appl Surf Sci 493:933–947. https://doi.org/10.1016/j.apsusc.2019.07.076
283. Xiao G, To S, Zhang G (2015) Molecular dynamics modelling of brittle–ductile cutting mode transition: case study on silicon carbide. Int J Mach Tools Manuf 88:214–222. https://doi.org/10.1016/j.ijmachtools.2014.10.007
284. Ivanov A, Cheng K (2019) Non-traditional and hybrid processes for micro and nano manufacturing. Int J Adv Manuf Technol 105:4481–4482. https://doi.org/10.1007/s00170-019-04711-0
285. Chavoshi SZ, Luo X (2015) Hybrid micro-machining processes: a review. Precis Eng 41:1–23. https://doi.org/10.1016/j.precisioneng.2015.03.001
286. Shen XH, Shi YL, Zhang JH et al (2020) Effect of process parameters on micro-textured surface generation in feed direction vibration assisted milling. Int J Mech Sci 167:105267. https://doi.org/10.1016/j.ijmecsci.2019.105267
287. Ko JH, Tan SW (2013) Chatter marks reduction in meso-scale milling through ultrasonic vibration assistance parallel to tooling's axis. Int J Precis Eng Manuf 14:17–22. https://doi.org/10.1007/s12541-013-0003-4
288. Ding H, Chen S-J, Cheng K (2011) Dynamic surface generation modeling of two-dimensional vibration-assisted micro-end-milling. Int J Adv Manuf Technol 53:1075–1079. https://doi.org/10.1007/s00170-010-2903-0
289. Kadivar M, Azrhoushang B, Zahedi A, Müller C (2019) Laser-assisted micro-milling of austenitic stainless steel X5CrNi18-10. J Manuf Process 48:174–184. https://doi.org/10.1016/j.jmapro.2019.11.002
290. Kim T, Kwon K-K, Chu CN, Song KY (2020) Experimental investigation on CO2 laser-assisted micro-slot milling characteristics of borosilicate glass. Precis Eng 63:137–147. https://doi.org/10.1016/j.precisioneng.2020.02.004
291. Carou D, Rubio EM, Herrera J et al (2017) Latest advances in the micro-milling of titanium alloys: a review. Procedia Manuf 13:275–282. https://doi.org/10.1016/j.promfg.2017.09.071
292. Kovács ZF, Viharos ZJ, Kodácsy J (2020) Surface flatness and roughness evolution after magnetic assisted ball burnishing of magnetizable and non-magnetizable materials. Measurement 158:107750. https://doi.org/10.1016/j.measurement.2020.107750
293. Huo D, Cheng K, Wardle F (2010) Design of a five-axis ultra-precision micro-milling machine—Ultramill. Part 1: holistic design approach, design considerations and specifications. Int J Adv Manuf Technol 47:867–877. https://doi.org/10.1007/s00170-009-2128-2
294. Cheng K, Huo D (2013) Micro cutting: fundamentals and applications. John Wiley & Sons, Chichester
295. Luo X, Cheng K, Webb D, Wardle F (2005) Design of ultraprecision machine tools with applications to manufacture of miniature and micro components. J Mater Process Technol 167:515–528. https://doi.org/10.1016/j.jmatprotec.2005.05.050
296. Zhang X, Yu T, Dai Y et al (2020) Energy consumption considering tool wear and optimization of cutting parameters in micro milling process. International Journal of Mechanical Sciences 105628. https://doi.org/10.1016/j.ijmecsci.2020.105628
297. Zhou C, Guo X, Zhang K et al (2019) The coupling effect of micro-groove textures and nanofluids on cutting performance of uncoated cemented carbide tools in milling Ti-6Al-4V. J Mater Process Technol 271:36–45. https://doi.org/10.1016/j.jmatprotec.2019.03.021
298. Rosli AM, Jamaludin AS, Razali MNM et al (2020) Modelling of fuzzy inference system for micro milling—a preliminary study through FEM. In: P. P. Abdul Majeed A, Mat-Jizat JA, Hassan MHA et al (eds) RITA 2018. Springer, Singapore, pp 445–456
299. Lu Y (2017) Industry 4.0: a survey on technologies, applications and open research issues. J Ind Inf Integr 6:1–10. https://doi.org/10.1016/j.jii.2017.04.005
300. Monostori L, Kádár B, Bauernhansl T et al (2016) Cyber-physical systems in manufacturing. CIRP Ann 65:621–641. https://doi.org/10.1016/j.cirp.2016.06.005
301. Jiang W (2014) Bio-inspired self-sharpening cutting tool surface for finish hard turning of steel. CIRP Ann 63:517–520. https://doi.org/10.1016/j.cirp.2014.03.047